cells. The present study revealed a novel function of autoAbs, which may contribute to the pathophysiology of BM failure.

Materials and Methods

Study subjects (patients)

Sera were obtained from 19 patients with AA and 4 healthy individuals. BM plasma was obtained from five patients with AA and three healthy individuals. All AA patients had severe AA and were positive for anti-moesin Abs. The samples were cryopreserved at −80°C until use. Peripheral blood (PB) was obtained from 7 patients with AA and 10 healthy individuals and BM was aspirated from 3 healthy individuals. The PBMCs were isolated using lymphoprep (Nycomed). All patients and healthy volunteers provided an informed consent before sampling according to the Declaration of Helsinki. This study was approved by the human research committee of Kanazawa University Graduate School of Medical Science.

Cell lines

Molt-4, THP-1, U937, K562, Daudi, and Jurkat cell lines were purchased from the Health Science Research Resources Bank. A megakaryoblastic leukemia cell line UT-7, a myeloid leukemia cell lines OUN-1, and a myelodysplastic syndrome cell line TF-1 were provided by Dr. N. Komatsu of Jichi Medical School, Dr. M.Yasukawa of Ehime University, and Dr. S. Ogawa of the University of Tokyo, respectively.

Purification of anti-moesin Abs in the sera of patients with AA

The anti-moesin polyclonal Abs (pAbs) were purified from the patients' serum with affinity chromatography using a protein G column (mAb Trap kit, no. 17-1128-0; GE Healthcare) and recombinant moesin protein (11) fixed on an agarose-gel column (1 ml, HiTrap NHS-activated HP, no. 17-0716-01; GE Healthcare) according to the manufacturer's instruction. In brief, 20 ml of serum from AA patients was applied to the Protein G column. After washing with the binding buffer, the whole IgG was eluted with the elution buffer and neutralized with the neutralizing buffer. The purified IgG was then applied to the recombinant moesin-fixed affinity chromatography column. After washing with the binding buffer (75 mM sodium phosphate (pH 8.0)), anti-moesin pAbs were eluted with the elution buffer (100 mM glycine-HCl and 500 mM NaCl (pH 2.7)). The purified anti-moesin pAbs were dialyzed in PBS at 4°C overnight using a spectra/Por Float-A-Lyzer column (Spectrum Laboratories; no. 235118). The purity of the isolated anti-moesin pAbs was confirmed by PAGE followed by Coomassie Brilliant Blue staining.

Flow cytometry

Mouse anti-moesin mAb (clone 38/87; Neomarkers) which was labeled with FITC (Immuno-Biological Laboratories) was used in combination with mAbs specific to CD3-PE (BD Pharmingen; no. 555333), CD19-PE (BD Pharmingen; No. 555413), CD4-PE (BD Pharmingen; No. 347327), CD-8-PE (BD Pharmingen; no. 555367), CD14-PE (BD Pharmingen; No. 555398), CD11b-PE (BD Pharmingen; No. 555388), CD34-PE (BD Pharmingen; no. 348057), and CD3-Cy-Chrome (BD Pharmingen; no. 555334). Isotype-matched control mAbs (BD Pharmingen) were used as negative controls. For the detection of moesin-like molecules on leukocytes and leukemia cell lines, 1 μl of anti-moesin mAbs and 2 μl of PE-labeled mAbs were added to 50 μl of cell suspension containing 1×10^6 cells and the suspension was incubated on ice for 30 min. For the detection of moesin-like molecules by pAbs, 1×10^6 THP-1 cells were washed twice with PBS containing 1% BSA (Sigma-Aldrich; no. A8022) and resuspended in 200 μl of a PBS containing 2% FCS, 2% goat serum, and 2% BSA. The cell suspension was incubated for 30 min at 4°C. Then, 5 μg/ml anti-moesin pAbs or isotype control human IgG pAbs isolated from healthy individuals were added to the cell suspension and incubated for 1 h at 4°C. The cells were washed twice with PBS containing 1% BSA followed by incubation with a secondary Ab (goat anti-human IgG FITC-labeled Ab; Sigma-Aldrich; no. F5512) diluted 1/100 in PBS containing 2% goat serum and were incubated at 4°C for 30 min. Finally, the cells were washed twice with PBS containing 1% BSA and subjected to flow cytometry.

Stimulation of THP-1 cells with PMA/LPS

THP-1 cells (10^6) were suspended in 2 ml of RPMI 1640 containing 10% FCS and 20 ng/ml PMA (Wako Chemicals; no. 545-00261) and incubated for 24 h at 37°C in a CO_2 incubator. A total of 10 ng/ml LPS (Sigma-Aldrich; no. L2880) was added to the cell suspension and further incubated for 20 h. The cultured cells were analyzed for the expression of moesin-like molecules by flow cytometry using anti-moesin mAbs (clone 38/87; Neomarkers).

Isolation of monocytes and T cells

Monocytes were isolated by plastic adherence as previously described (20). In brief, 5×10^6 PBMCs/well were distributed into 12-well plates (Corning) and allowed to adhere in a 5% CO_2 incubator at 37° for 2 h in RPMI 1640 supplemented with 10% (v/v) heat-inactivated FCS, 100 U/ml penicillin - 0.1 mg/ml streptomycin (Invitrogen; No.15140-148) and 10 μg/ml polymyxin B (Aerosporin) (Sigma-Aldrich; no. 194538). Nonadherent cells were removed and the remaining adherent cells on the plates were used as monocytes. T cells were purified by negative selection using the Human T Cell Enrichment Columns (R&D Systems; no. HTCC-500) following the manufacturer instructions. The purity of enriched T cells and monocytes was approximately 90% as determined by flow cytometry using anti-CD3-PE and anti-CD-14-PE mAbs, respectively.

Stimulation of THP-1 cells, PBMCs, monocytes, and T cells with anti-moesin Abs

THP-1 cells, PBMCs, monocytes, or T cells were suspended in RPMI 1640 supplemented with 10% (v/v) heat-inactivated FCS. Polymyxin B (Aerosporin) (Sigma-Aldrich; no. 194538) was added at 10 μg/ml to eliminate any contaminating endotoxin. The endotoxin concentration in the pAbs and the reagents used for culture was <10 pg/ml as demonstrated by chromogenic *Limulus* amebocyte lysate assay (Seikagaku). The cells (5×10^5) were incubated for 48 h in the presence of 5 μg/ml of anti-moesin mouse mAbs (clone 38/87, IgG1; Neomarkers) or 5–10 μg/ml of pAbs isolated from the serum of AA patients as described above. Mouse mAbs (Coulter Clone; IgG1, no. 6602872) and control human IgG pAbs isolated from healthy individuals were used as negative controls. This Ab concentration was selected based on an estimated concentration of anti-moesin pAbs in the serum of an AA patient. For prestimulation of PBMCs to induce IFN-γ secretion, the cells were incubated for 1 h in the presence of 100 ng/ml of anti-CD3 mAbs (Clone OKT3) (eBioscience; functional grade no. 16-0037). For co-stimulation of isolated T cells to induce IFN-γ secretion, the cells were cultured for 48 h on a 48-well tissue culture plate that was coated with 100 ng/ml of anti-CD3 mAbs (clone OKT3) (eBioscience; functional grade no. 16-0037) overnight at 4°C and washed. Then, 100 ng/ml LPS or 10 μg/ml PHA (Sigma-Aldrich; no. L4144) was included instead of anti-moesin Abs as the positive controls for the induction of TNF-α or IFN-γ secretion, respectively, and control human IgG pAbs isolated from healthy individuals were added as a negative control.

Western blotting

Western blotting was performed using THP-1 cell lysates. The specific bands were visualized by anti-moesin mAbs, pAbs from AA patients, or control human IgG pAbs from healthy individuals as described in a previous report (11). The expression levels of α-tubulin were determined as an internal control using Western blotting with anti-α-tubulin mAbs (Sigma-Aldrich; no. T 5168).

Isolation of proteins on the surface of THP-1 cells

The THP-1 cells were treated with sulfo-NHS-SS-biotin, and the cell surface proteins were isolated with avidin-fixed columns according to the manufacturer's instructions (Pierce). Thereafter, 1×10^7 cells were washed twice with 8 ml of ice-cold PBS. The cells were suspended in 10 ml PBS containing 2.5 mg sulfo-NHS-SS-Biotin and incubated for 30 min at 4°C. Then, 500 μl of quenching solution was added to the cell suspension and the cells were washed with 10 ml TBS twice. The cell pellet was lysed in 500 μl of lysis buffer containing 60 μl of preotease inhibitor cocktail (Sigma-Aldrich; no. P-8340) and then disrupted by sonication. The biotin-labeled membrane proteins were isolated by an immobilized NeutrAvidin Gel column. The isolated membrane proteins were subjected to Western blotting and peptide mass fingerprinting.

Peptide mass fingerprinting

Mass spectrometric identification of 80- and 75-kDa proteins on the surface of the THP-1 cells was performed as previously described (21). In brief, the proteins fractionated by SDS-PAGE were visualized by Coomassie Brilliant Blue staining and the 80- and 75-kDa bands were excised from gels, followed by in-gel digestions with trypsin (Promega) in a buffer containing 50 mM ammonium bicarbonate (pH 8.0) and 2% acetonitrile overnight at 37°C. Molecular mass analyses of the tryptic

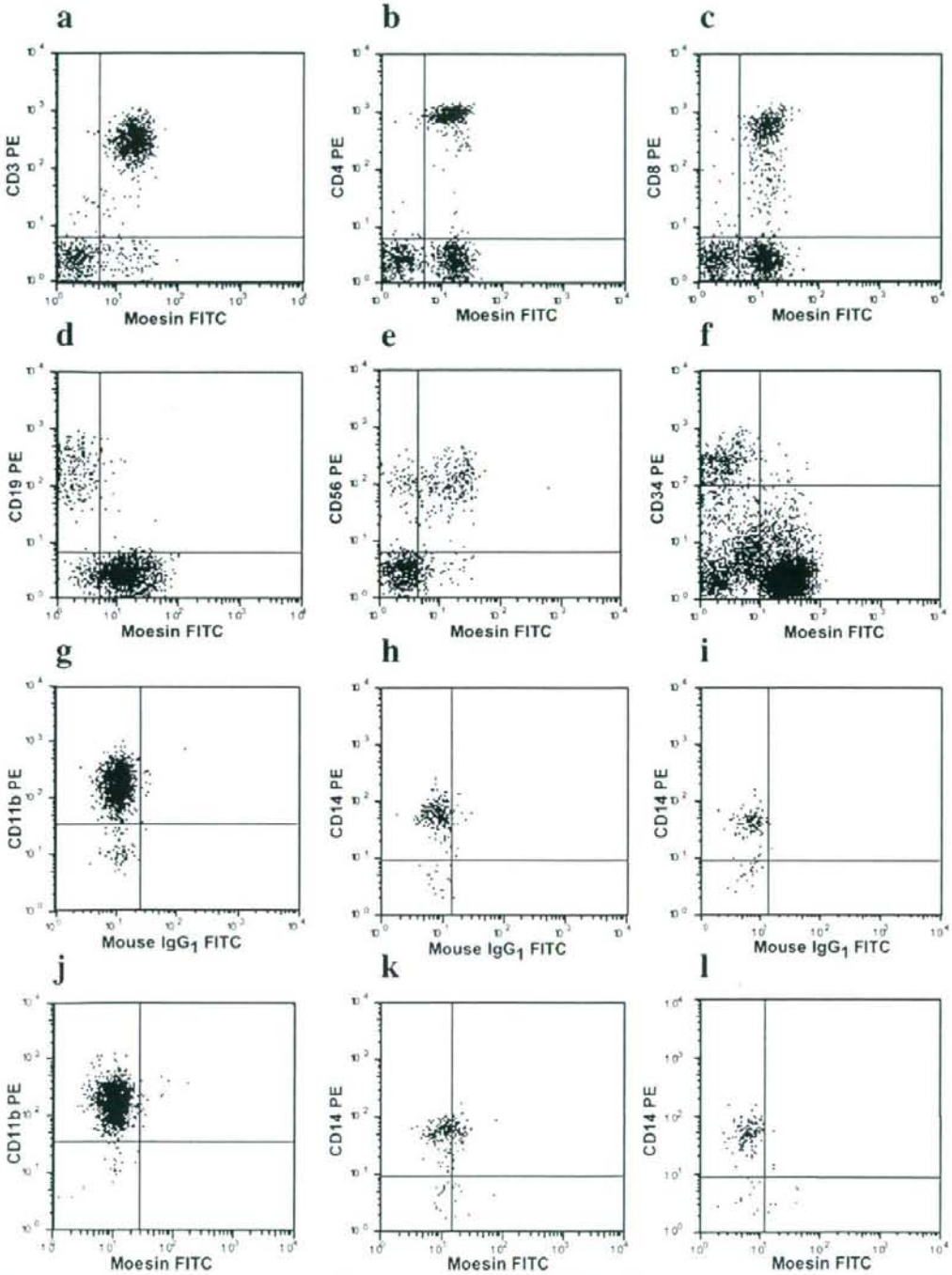

FIGURE 1. Expression of moesin-like molecules on the surface of various blood cells. PB lymphocytes, granulocytes, and monocytes, as well as BM mononuclear cells, of a healthy individual and a patient with AA were analyzed by flow cytometry. The gate was set up for lymphocytes (*a–d*), $CD3^-$ lymphocytes (*e*), granulocytes (*g* and *j*), and monocytes (*h* and *k*) derived from a healthy individual and monocytes (*i* and *l*) derived from an AA patient. BM mononuclear cells (*f*) of a healthy individual were included in the analysis. One representative result of three experiments is shown.

peptides were performed by matrix-assisted laser desorption/ionization time-of-flight mass spectrometry using an ultraflex TOF/TOF (Bruker Daltonics). The proteins were identified by comparisons between the molecular weights determined by matrix-assisted laser desorption/ionization time-of-flight mass spectrometry and the theoretical peptide masses of proteins registered in NCBInr.

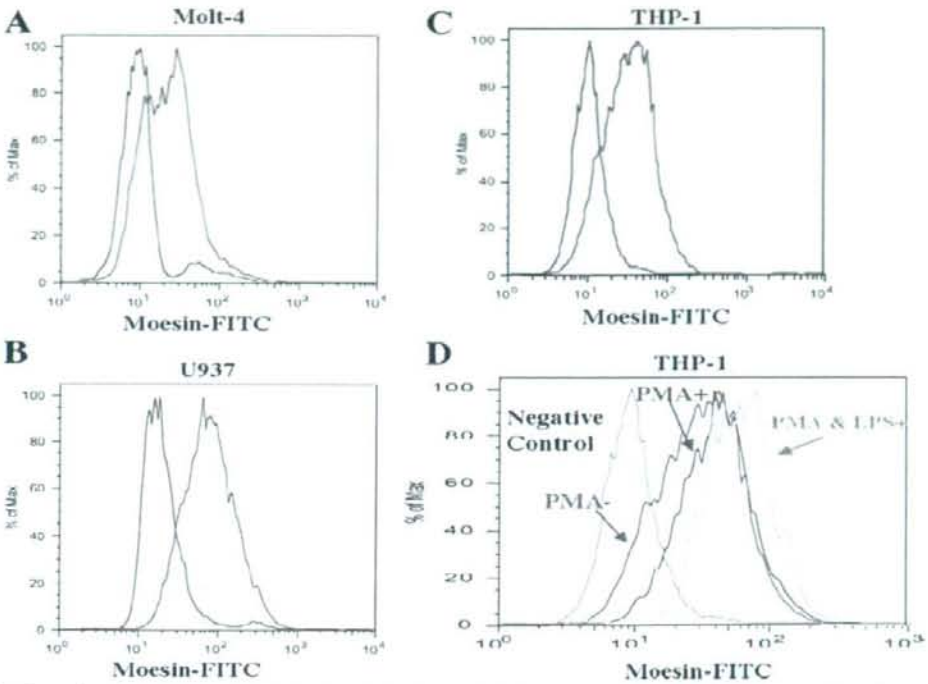

FIGURE 2. Expression of moesin-like molecules on the surface of T cell and monocytic leukemia cell lines. *A–C*, Three leukemia cell lines were examined for the cell surface expression of moesin-like molecules. Left lines, mouse IgG used as negative control; right lines, FITC-labeled anti-moesin mAbs. *D*, THP-1 cells were cultured in the presence or absence of 20 ng/ml PMA for 24 h and then the PMA-stimulated cells were further cultured in the presence of 10 ng/ml LPS for 20 h. The cultured cells were analyzed for the expression of moesin-like molecules by flow cytometry. One representative result is shown.

Transfection of moesin short hairpin (shRNA)

Moesin shRNA plasmid (pENTR/moesin-shRNA-264) (22) was kindly provided by Dr. G. M. Kelly of the University of Western Ontario (Ontario, Canada). THP-1 cells were transfected by electroporation using a Gene Pulser II Electroporation System (Bio-Rad). In brief, 3–5 μg of moesin shRNA plasmid or control shRNA (pENTR/U6-GW/lacZ^{shRNA}) was mixed with 800 μl of Opti-Mem I medium (Invitrogen) containing 1×10^6 THP-1 cells and incubated on ice for 10 min. The cells were electroporated in a 4-mm cuvette (Bio-Rad) at the setting of 300 V of voltage pulse and 960 μF of capacitance. Immediately after electroporation, the transfected THP-1 cells were left on ice for 10 min and then 3 ml of RPMI 1640 containing 10% FCS was added to the cell suspension followed by overnight incubation at 37°C. The cells were rinsed and cultured in 3 ml of fresh RPMI 1640 containing 10% FCS for 72 h at 37°C in a CO_2 incubator and were analyzed for the expression of moesin-like molecules by flow cytometry using FITC-labeled anti-moesin mAb (clone 38/87; Neomarkers).

ELISA

The TNF-α and IFN-γ concentration in the culture supernatant, as well as in PB serum and BM plasma was measured using ELISA kits (Mabtech;

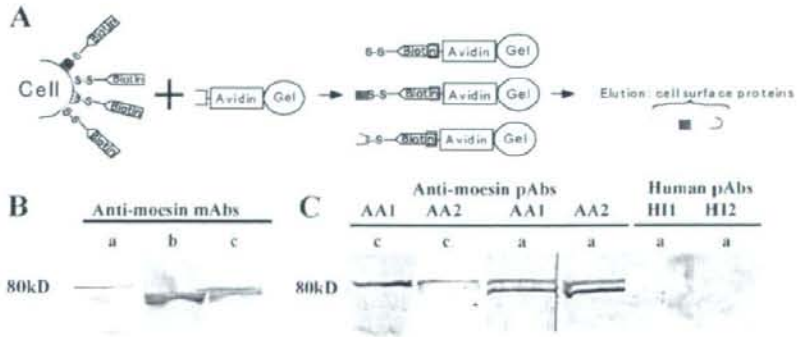

FIGURE 3. Isolation and identification of proteins on THP-1 cells recognized by anti-moesin Abs. *A*, THP-1 cells were treated with sulfo-NHS-SS-biotin and the cell surface proteins were isolated with avidin-fixed columns. *B*, Three different protein lysates (*a*, whole cells; *b*, cytoplasmic proteins; and *c*, surface proteins) were subjected to Western blotting with anti-moesin mAbs. *C*, THP-1 cell lysates (*a*) and surface proteins (*c*) isolated from THP-1 cells were subjected to Western blotting using anti-moesin pAbs purified from two AA patients' sera (AA1 and AA2) or non-specific control human IgG pAbs purified from two healthy individuals' sera (HI1 and HI2).

AB, No. 3510-1H-20, and Mabtech; AB, No. 3420-1H-6) according to the manufacturer's instructions. The OD absorbance at 450 nm was determined using a SLTEAR 340 ATELISA reader (SLT-Labinstruments). For determination of cytokine levels in the PB serum and BM plasma, the following additional procedures were performed. Samples were centrifuged at 10,000 rpm for 10 min. ELISA plates were covered with 200 μl/well of TNF-α assay diluent (eBioscience; No. 00-4202-AD) or IFN-γ assay diluent (Mabtech; No. 3652-D) for 1 h at room temperature before adding samples to block nonspecific reactions. TNF-α assay diluent (eBioscience; No. 00-4202-AD) and IFN-γ assay diluent (Mabtech; No. 3652-D) were used to dilute biotinylated mAb TNF-α-II solution and biotinylated mAb 7-B6-1, respectively.

Statistics

The results are given as the mean ± SD. Comparisons were made using the paired *t* test.

Results

Expression of moesin-like molecules on the surface of various blood cells

To confirm the expression of moesin-like molecules on the PB and BM cells, various leukocyte subsets were examined using flow cytometry with anti-moesin mAbs. Fig. 1 shows the representative results of flow cytometry on one healthy individual. Moesin-like molecules were detectable on T cells, NK cells, and monocytes on their surface but not on B cells, neutrophils, and BM $CD34^+$ cells as shown in Fig. 1. All three healthy individuals and the three AA patients showed similar results except that moesin-like molecules were not detectable on monocytes derived from the three AA patients. The mean fluorescence intensity values of the monocytes from healthy individuals and AA patients were 11.5 ± 2.2 and 6.6 ± 2.1, respectively, and the difference was significant (mean fluorescence intensity ± SD, $p < 0.05$, unpaired *t* test). In addition to the leukocyte subsets from the healthy individuals, moesin-like molecules were detectable on a T cell leukemia cell line Molt-4 as well as on monocytic leukemia cell lines U937 and THP-1 (Fig. 2), while they were undetectable on myeloid leukemia cell lines such as K562, UT-7, OUN-1, and TF-1. They were either undetectable on the Burkitt lymphoma cell line, Daudi, or T cell lymphoma cell line, Jurkat (data not shown). The treatment of THP-1 with 20 ng/ml PMA for 24 h and/or 10 ng/ml LPS for 20 h augmented the expression of moesin-like molecules (Fig. 2*D*), thus, indicating an up-regulation of the moesin-like molecules associated with the differentiation of THP-1 cells into macrophages.

Identification of moesin on the surface of THP-1 cells

To identify the proteins on THP-1 cells recognized by anti-moesin Abs, the THP-1 cells were treated with sulfo-NHS-SS-biotin and the cell surface proteins were isolated with avidin-fixed columns (Fig. 3*A*). Western blotting of the isolated proteins with anti-moesin mAbs showed two clear bands of which the sizes were 75 and 80 kDa (Fig. 3*B*). Mass fingerprinting of the eluted protein revealed the 80 kDa protein to be moesin. The 75 kD band proved to be nucleolin and eukaryotic translation elongation factor 2. To confirm that anti-moesin pAbs in the serum of AA patients can bind to this cell surface moesin, anti-moesin pAbs were purified from the AA patients' sera (AA1 and AA2) with recombinant moesin proteins using affinity chromatography and then were used for Western blotting. As shown in Fig. 3*C*, the serum-derived anti-moesin pAbs bound to moesin derived from the surface proteins of THP-1.

Effect of moesin-specific shRNA on the expression of moesin on THP-1 cells

To further confirm the expression of moesin on the surface of THP-1 cells, the cells were transfected with moesin shRNA using electroporation. Flow cytometry showed a decrease in the moesin expression level on the surface of the THP-1 cells transfected with moesin shRNA in comparison to the THP-1 cells transfected with negative control shRNA (Fig. 4*A*). When the THP-1 cells transfected with different dosages of moesin-specific shRNA were examined by Western blotting, the moesin expression by the THP-1 cells was decreased in a dose-dependent manner. The control shRNA specific to LacZ had no effect on moesin expression.

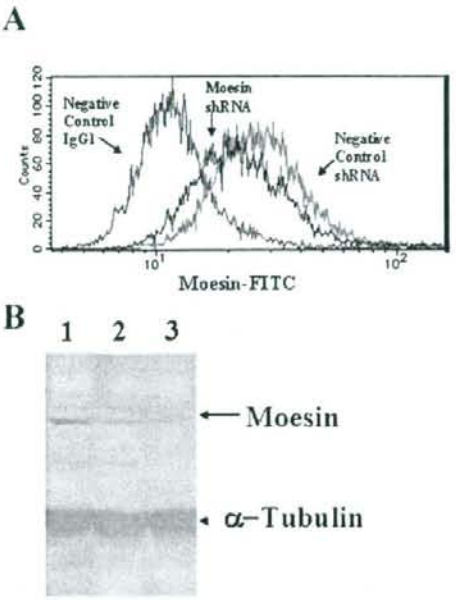

FIGURE 4. Effect of moesin shRNA transfection on the expression of moesin by THP-1 cells. *A*, THP-1 cells transfected with 5 μg of moesin shRNA or control shRNA were examined for the expression of moesin with flow cytometry. The blue line, non-transfected THP-1 cells stained with control mouse IgG1 mAbs; the green line, moesin shRNA transfected cells stained with anti-moesin IgG1 mAbs; the red line, negative control shRNA transfected cells stained with anti-moesin IgG1 mAbs. *B*, Negative control shRNA or moesin-specific shRNA transfected THP-1 cell lysates were examined by Western blotting. 1, 5 μg control shRNA; 2, 3 μg moesin shRNA; 3, 5 μg moesin shRNA.

Effect of anti-moesin Abs on THP-1 cells

To determine whether anti-moesin Abs have some effects on THP-1 cells, the THP-1 cells were cultured in the presence of anti-moesin Abs or control IgG for 48 h and the TNF-α concentration of the culture supernatant was measured using ELISA. Both the anti-moesin mAbs and pAbs induced a significantly greater amount of TNF-α from the THP-1 cells than did the control IgG (Fig. 5*A*). The amount of TNF-α induced by anti-moesin pAbs (5 μg/ml) was almost comparable to that induced by LPS (100 ng/ml) (Fig. 5*A*). The anti-moesin pAbs' binding to moesin on the THP-1 cells was ascertained by flow cytometry (Fig. 5*B*).

Effect of anti-moesin pAbs on PBMCs, monocytes, and T cells from healthy individuals and AA patients

The expression of moesin on the T cells and monocytes as well as the TNF-α secretion from the THP-1 cells induced by anti-moesin pAbs suggested that anti-moesin pAbs in the AA patients' sera might also stimulate these immune cells from healthy individuals and AA patients to secrete cytokines. When the PBMCs from healthy individuals were incubated for 48 h in the presence of 5

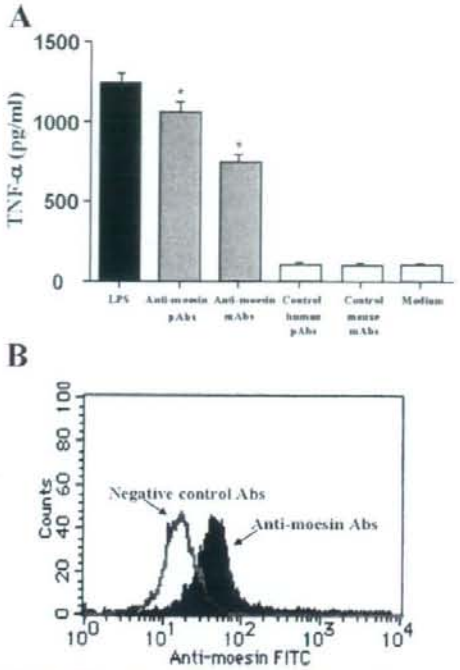

FIGURE 5. TNF-α release from THP-1 cells stimulated by anti-moesin Abs. *A*, THP-1 cells were cultured for 48 h with 5 μg/ml of anti-moesin Abs or control Abs. Anti-moesin pAbs, anti-moesin polyclonal IgG isolated from the serum of AA patients; control human pAbs, control human IgG pAbs isolated from healthy individuals; anti-moesin mAbs, anti-moesin mouse IgG1 mAbs (clone 38/87); control mouse mAbs, control mouse IgG1 mAbs. Then, 100 ng/ml LPS was used as a positive control. The data represent the mean TNF-α concentration ± SD of three experiments. *, $p < 0.01$ vs control Abs. *B*, The detection of moesin on THP-1 cells by anti-moesin pAbs purified from the serum of an AA patient.

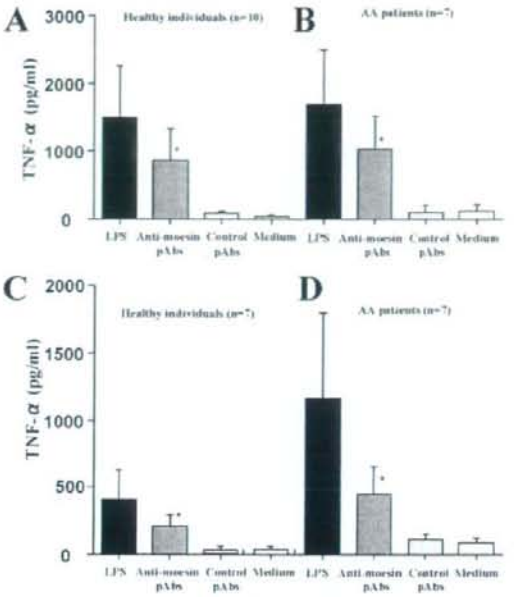

FIGURE 6. TNF-α release from PBMCs or monocytes stimulated by anti-moesin pAbs. The PBMCs or isolated monocytes were cultured for 48 h in the presence of 5 μg/ml of anti-moesin IgG pAbs or human control IgG pAbs isolated from the serum of AA patients or healthy individuals. Then, 100 ng/ml of LPS was used as a positive control. PBMCs isolated from 10 healthy individuals (*A*) and 7 AA patients (*B*), and monocytes separated from the PBMCs of 7 healthy individuals (*C*) and 7 AA patients (*D*), were used as targets. The data represent the mean TNF-α concentration ± SD. *, $p < 0.005$ vs control Abs.

μg/ml of anti-moesin pAbs, the amount of TNF-α in the culture medium was approximately 10 times more than those of control cultures and was more than half of that of the culture stimulated by 100 ng/ml of LPS (Fig. 6*A*). The same concentration of anti-moesin pAbs induced a similar amount of TNF-α from the PBMCs from AA patients (Fig. 6*B*). On the other hand, when monocytes isolated from the PBMC of healthy individuals or AA patients were used as a target, anti-moesin pAbs induced less than half the amount of TNF-α of that induced from whole PBMCs (Fig. 6, *C* and *D*).

The unexpectedly high inducibility of TNF-α secretion from the PBMCs by the anti-moesin pAbs prompted studies on the inducibility of IFN-γ secretion from the PBMCs by the Abs. Fig. 7, *A* and *B*, shows the effect of anti-moesin Abs on the IFN-γ secretion from PBMCs. Although anti-moesin pAbs alone could not induce IFN-γ secretion from the PBMCs derived from healthy individuals, the Abs stimulated PBMCs that were prestimulated with anti-CD3 mAbs to secrete nearly as much IFN-γ as that PHA did. In contrast, the PBMCs from the AA patients could secrete IFN-γ in response to anti-moesin pAbs without the prestimulation by anti-CD3 mAbs, and the amount of IFN-γ was approximately 40% as much as that of the culture stimulated by 10 μg/ml of PHA. In contrast, T cells isolated from the PBMC of healthy individuals or AA patients could not secrete a significantly larger amount of IFN-γ in response to anti-moesin pAbs compared with that in response to control IgG pAbs (Fig. 7, *C* and *D*), and the amount of IFN-γ secreted by T cells was one-tenth as much as that by PBMCs.

When the sera of the 16 AA patients comprising 7 anti-moesin Ab-positive and 9 anti-moesin Ab-negative patients were examined using ELISA, no significant differences in TNF-α and IFN-γ concentrations were observed between the 2 groups (TNF-α: 88.0 ± 106.3 pg/ml in anti-moesin Abs-positive patients, 90.1 ± 161.3 in anti-moesin Abs-negative patients; IFN-γ: 44.6 ± 33.8 pg/ml in anti-moesin Abs-positive patients, 47.5 ± 44.9 pg/ml in anti-moesin Abs-negative patients). None of the sera derived from four healthy donors showed detectable levels of TNF-α (>5 pg/ml) and IFN-γ (>5 pg/ml). On the other hand, when the BM plasma from five patients with AA was examined using ELISA, three anti-moesin Abs-positive patients showed higher levels of TNF-α (129, 338, and 349 pg/ml) compared with those of TNF-α (13 and 128 pg/ml) in two anti-moesin Abs-negative patients. IFN-γ concentrations of three anti-moesin Abs-positive patients were 29, 123, and 133 pg/ml, while those of two anti-moesin Abs-negative patients were 13 and 80 pg/ml. None of the BM plasma derived from three healthy donors showed detectable levels of TNF-α (>5 pg/ml) and IFN-γ (>5 pg/ml).

Discussion

The present study revealed that the proteins recognized by the anti-moesin Abs are detectable on the surface of various leukocytes subsets including T cells, NK cells, and monocytes as well as on T lymphocytic and monocytic leukemia cell lines. Moesin is an intracellular protein that links the cell membrane and cytoskeleton, and mediates the formation of microtubules and cell adhesion sites

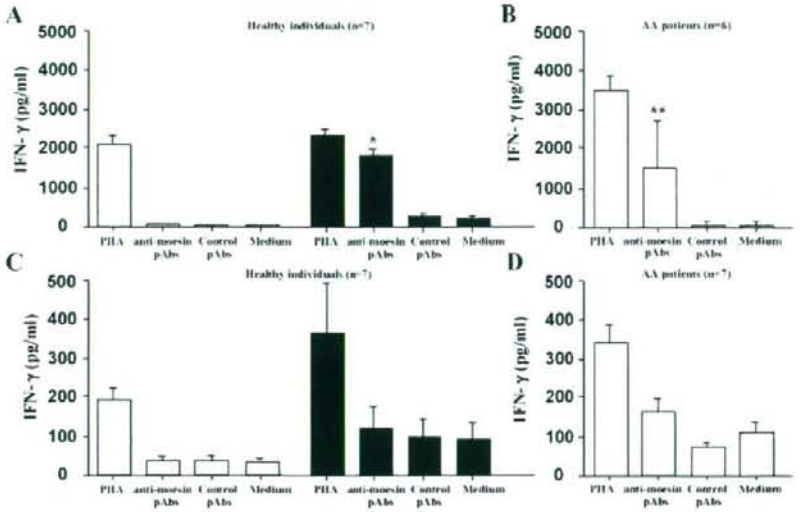

FIGURE 7. IFN-γ release from PBMCs or T cells stimulated by anti-moesin Abs. The PBMCs or isolated T cells were cultured for 48 h in the presence of 5 μg/ml of anti-moesin IgG pAbs or human control IgG pAbs isolated from the serum of AA patients or healthy individuals. Then, 10 μg/ml PHA was used as a positive control. Unprimed PBMCs (□) or CD3-primed PBMCs (■) were used for the culture. PBMCs were isolated from seven healthy individuals (*A*) and six AA patients (*B*). Uncostimulated T cells (□) or CD3-costimulated T cells (■) were used for the culture. T cells were isolated from the PBMCs of seven healthy individuals (*C*) and seven AA patients (*D*). The data represent the mean IFN-γ concentration ± SD. *, $p < 0.0001$ vs control Abs; **, $p = 0.04$ vs control Abs.

as well as ruffling of the cell membrane (17). This membrane-linking protein is expressed by various blood cells including megakaryocytes and granulocytes (23), but its expression was thought to be localized inside the cell membrane and not on the cell surface. Some studies revealed that anti-moesin Abs could bind to the surface of T cells (18) and macrophages (19) in keeping with our observation. However, none of the previous studies characterized the cell surface protein recognized by the anti-moesin Abs. Using biotin-labeled membrane proteins coupled with an avidin gel column and peptide massfinger printing, the present study identified the cell surface 80 kDa protein to be moesin. The decrease in the cell surface moesin induced by moesin shRNA has substantiated the presence of moesin on the cell surface of THP-1 cells.

Little is known about the function of anti-moesin Abs in vitro and in vivo. In contrast to our results, Amar et al. (24, 25) found that anti-moesin mAbs (clone 38) suppressed LPS-induced TNF-α secretion from monocytes through binding of moesin-like molecules on the cell surface. They used a different anti-moesin mAbs (clone 38) from the mAbs (clone 38/87) used in the present study. When we examined the effect of clone 38 mAbs on TNF-α secretion from THP-1 cells induced by LPS using the same condition as the one described by Amar et al. (24), a dose-dependent inhibition of TNF-α secretion was observed (data not shown). In contract to clone 38/87 mAb and pAbs from AA patients' sera, the clone 38 mAbs alone did not induce TNF-α secretion from THP-1 cells. Because the clone 38 preparation contains 1.5 mM sodium azide as a preservative, it is most likely that the dose-dependent inhibition of TNF-α secretion by clone 38 mAbs was due to toxic effect of sodium azide. Alternatively, clone 38 mAb which recognizes the C-terminal portion (554–564 amino acid residues) of moesin may exert a different effect on THP-1 cells from the effect of mAb clone 38/87 which recognizes the middle portion (317–398 amino acid residues) of moesin and from the effect of pAbs purified from AA patients' sera.

The present study revealed that both mAbs and pAbs specific to moesin stimulated the THP-1 cells to secrete TNF-α at an Ab concentration compatible to that in the serum of the AA patients. Moreover, anti-moesin pAbs were as potent as LPS in inducing TNF-α secretion from the PBMCs derived from healthy individuals and the AA patients. Our preliminary analyses on the activation of signaling pathways leading to TNF-α secretion from THP-1 cells showed the phosphorylation of ERK1/2 kinase induced by anti-moesin Abs (49th American Society of Hematology annual meeting abstract #1690, 2007 and submitted). In two patients from whom anti-moesin pAbs were purified, the Abs induced TNF-α release from autologous PBMCs. High concentrations of TNF-α were indeed present in the BM sera of two patients with high anti-moesin Ab titer. Although no difference in the serum TNF-α level was observed between anti-moesin Ab-positive and -negative patients, these findings suggest that anti-moesin Abs may induce a subtle amount of TNF-α from the monocytes or macrophages in the BM, thereby contributing to the pathogenesis of AA.

In contrast to TNF-α, IFN-γ was not induced by the anti-moesin pAbs alone from the PBMCs from healthy individuals, though anti-moesin pAbs augmented IFN-γ secretion from the PBMCs prestimulated with anti-CD3 mAbs. On the other hand, anti-moesin pAbs stimulated the PBMCs from the AA patients to secrete as much IFN-γ as did PHA. It has been shown that T cells from AA patients are in an activated state and are prone to produce IFN-γ in response to suboptimal stimuli (26). The amount of secreted TNF-α from isolated monocytes as well as the amount of secreted IFN-γ from isolated T cells was greatly reduced compared with those from unfractionated PBMCs. The inability to secrete a sufficient amount TNF-α and IFN-γ of isolated monocytes and T cells suggests that the interaction between monocytes and T cells may be required to efficiently respond to extrinsic stimuli as described by previous reports (27, 28). When the anti-moesin Abs titers in the serum were longitudinally measured in three patients, the Abs titer decreased in two patients in association with the response to immunosuppressive therapy, while the Abs titer increased in one patient who became dependent on transfusions due to the relapse of AA in comparison to the titer detected in remission (data not shown). The high titer TNF-α levels in BM plasma of patients showing high anti-moesin Abs titers and the decrease in the Ab titers in parallel with disease amelioration support the hypothesis that anti-moesin Abs are involved in the pathogenesis of AA by way of myelosuppressive cytokine induction from immunocompetent cells. One may wonder why high titer anti-moesin Abs in some AA patients do not induce hypercytokinemia. However, inability of T cell-stimulating Abs such as anti-CD3 Abs to induce IFN-γ secretion in vivo has been shown by previous reports (29, 30). There may be some regulatory mechanisms that mitigate T cell activation by stimulating Abs in vivo.

A previous study demonstrated the presence of anti-moesin Abs in 14–34% of patients with rheumatoid arthritis (11, 31), and a

case-control study on AA conducted by the International Agranulocytosis and Aplastic Anemia Study Group revealed that a past history of rheumatoid arthritis is significantly associated with the later development of AA (32). The anti-moesin pAbs derived from patients with rheumatoid arthritis also enhanced TNF-α secretion from THP-1 cells (data not shown). It is, therefore, possible that AA and rheumatoid arthritis may share pathogenetic mechanisms leading to a breakdown of immunologic tolerance to moesin. Anti-TNF-α therapy has been successfully used for patients with rheumatoid arthritis (33–35) as well as for some patients with myelodysplastic syndrome (36, 37). Recent reports have shown the efficacy of anti-CD20 Abs in restoring hematopoietic functions of AA (38, 39). Therefore, autoAbs capable of inducing cytokine secretion like anti-moesin Abs may be a new target of therapy for AA.

Acknowledgments

We gratefully acknowledge Prof. A. Yachie of Kanazawa University for suggestions and helpful discussion. We also thank M. Yoshii, A. Hamano, R. Oumi, and T. Tanaka of Cellular Transplantation Biology of Kanazawa University for technical assistance.

Disclosures

The authors have no financial conflict of interest.

References

1. Young, N. S. 2002. Acquired aplastic anemia. *Ann. Intern. Med.* 136: 534–546.
2. Bacigalupo, A., G. Broccia, G. Corda, W. Arcese, M. Carotenuto, A. Gallamini, F. Locatelli, P. G. Mori, P. Saracco, G. Todeschini, et al. 1995. Antilymphocyte globulin, cyclosporin, and granulocyte colony-stimulating factor in patients with acquired severe aplastic anemia (SAA): a pilot study of the EBMT SAA Working Party. *Blood* 85: 1348–1353.
3. Rosenfeld, S. J., J. Kimball, D. Vining, and N. S. Young. 1995. Intensive immunosuppression with antithymocyte globulin and cyclosporine as treatment for severe acquired aplastic anemia. *Blood* 85: 3058–3065.
4. Hoffman, R., E. D. Zanjani, J. D. Lutton, R. Zalusky, and L. R. Wasserman. 1977. Suppression of erythroid-colony formation by lymphocytes from patients with aplastic anemia. *N. Engl. J. Med.* 296: 10–13.
5. Nissen, C., P. Cornu, A. Gratwohl, and B. Speck. 1980. Peripheral blood cells from patients with aplastic anemia in partial remission suppress growth of their own bone marrow precursors in culture. *Br. J. Haematol.* 45: 233–243.
6. Nakao, S., A. Takami, H. Takamatsu, W. Zeng, N. Sugimori, H. Yamazaki, Y. Miura, M. Ueda, S. Shiobara, T. Yoshioka, et al. 1997. Isolation of a T-cell clone showing HLA-DRB1*0405-restricted cytotoxicity for hematopoietic cells in a patient with aplastic anemia. *Blood* 89: 3691–3699.
7. Zeng, W., J. P. Maciejewski, G. Chen, and N. S. Young. 2001. Limited heterogeneity of T cell receptor BV usage in aplastic anemia. *J. Clin. Invest.* 108: 765–773.
8. Hirano, N., M. O. Butler, M. S. Von Bergwelt-Baildon, B. Maecker, J. L. Schultze, K. C. O'Connor, P. H. Schur, S. Kojima, E. C. Guinan, and L. M. Nadler. 2003. Autoantibodies frequently detected in patients with aplastic anemia. *Blood* 102: 4567–4575.
9. Feng, X., T. Chuhjo, C. Sugimori, T. Kotani, X. Lu, A. Takami, H. Takamatsu, H. Yamazaki, and S. Nakao. 2004. Diazepam-binding inhibitor-related protein 1: a candidate autoantigen in acquired aplastic anemia patients harboring a minor population of paroxysmal nocturnal hemoglobinuria-type cells. *Blood* 104: 2425–2431.
10. Hirano, N., M. O. Butler, E. C. Guinan, L. M. Nadler, and S. Kojima. 2005. Presence of anti-kinectin and anti-PMS1 antibodies in Japanese aplastic anaemia patients. *Br. J. Haematol.* 128: 221–223.
11. Takamatsu, H., X. Feng, T. Chuhjo, X. Lu, C. Sugimori, K. Okawa, M. Yamamoto, S. Iseki, and S. Nakao. 2007. Specific antibodies to moesin, a membrane-cytoskeleton linker protein, are frequently detected in patients with acquired aplastic anemia. *Blood* 109: 2514–2520.
12. Weetman, A. P. 2003. Grave's disease 1835–2002. *Horm. Res.* 59 (*Suppl.* 1): 114–118.
13. Kitajima, Y., and Y. Aoyama. 2007. A perspective of pemphigus from bedside and laboratory-bench. *Clin. Rev. Allergy Immunol.* 33: 57–66.
14. Baroni, S. S., M. Santillo, F. Bevilacqua, M. Luchetti, T. Spadoni, M. Mancini, P. Fraticelli, P. Sambo, A. Funaro, A. Kazlauskas, et al. 2006. Stimulatory autoantibodies to the PDGF receptor in systemic sclerosis. *N. Engl. J. Med.* 354: 2667–2676.
15. Svegliati, S., A. Olivieri, N. Campelli, M. Luchetti, A. Poloni, S. Trappolini, G. Moroncini, A. Bacigalupo, P. Leoni, E. V. Avvedimento, and A. Gabrielli. 2007. Stimulatory autoantibodies to PDGF receptor in patients with extensive chronic graft-versus-host disease. *Blood* 110: 237–241.
16. Ralston, D. R., C. B. Marsh, M. P. Lowe, and M. D. Wewers. 1997. Antineutrophil cytoplasmic antibodies induce monocyte IL-8 release: role of surface proteinase-3, α1-antitrypsin, and Fcγ receptors. *J. Clin. Invest.* 100: 1416–1424.
17. Tsukita, S., and S. Yonemura. 1999. Cortical actin organization: lessons from ERM (ezrin/radixin/moesin) proteins. *J. Biol. Chem.* 274: 34507–34510.
18. Ariel, A., R. Hershkoviz, I. Altbaum-Weiss, S. Ganor, and O. Lider. 2001. Cell surface-expressed moesin-like receptor regulates T cell interactions with tissue components and binds an adhesion-modulating IL-2 peptide generated by elastase. *J. Immunol.* 166: 3052–3060.
19. Matsuyama, A., N. Sakai, H. Hiraoka, K. Hirano, and S. Yamashita. 2006. Cell surface-expressed moesin-like HDL/apoA-I binding protein promotes cholesterol efflux from human macrophages. *J. Lipid Res.* 47: 78–86.
20. Elkord, E., P. E. Williams, H. Kynaston, and A. W. Rowbottom. 2005. Human monocyte isolation methods influence cytokine production from in vitro generated dendritic cells. *Immunology* 114: 204–212.
21. Jensen, O. N., A. Podtelejnikov, and M. Mann. 1996. Delayed extraction improves specificity in database searches by matrix-assisted laser desorption/ionization peptide maps. *Rapid Commun. Mass Spectrom.* 10: 1371–1378.
22. Krawetz, R., M. J. MacKenzie, Q. Sun, P. A. Walton, and G. M. Kelly. 2006. Gα13 activation rescues moesin-depletion induced apoptosis in F9 teratocarcinoma cells. *Exp. Cell. Res.* 312: 3224–3240.
23. Masumoto, J., J. Sagara, M. Hayama, E. Hidaka, T. Katsuyama, and S. Taniguchi. 1998. Differential expression of moesin in cells of hematopoietic lineage and lymphatic systems. *Histochem. Cell Biol.* 110: 33–41.
24. Amar, S., K. Oyaisu, L. Li, and T. Van Dyke. 2001. Moesin: a potential LPS receptor on human monocytes. *J. Endotoxin Res.* 7: 281–286.
25. Tohme, Z. N., S. Amar, and T. E. Van Dyke. 1999. Moesin functions as a lipopolysaccharide receptor on human monocytes. *Infect. Immun.* 67: 3215–3220.
26. Solomou, E. E., K. Keyvanfar, and N. S. Young. 2006. T-bet, a Th1 transcription factor, is up-regulated in T cells from patients with aplastic anemia. *Blood* 107: 3983–3991.
27. Debets, J. M., C. J. van der Linden, I. E. Spronken, and W. A. Buurman. 1988. T cell-mediated production of tumour necrosis factor-α by monocytes. *Scand. J. Immunol.* 27: 601–608.
28. Tsukaguchi, K., B. de Lange, and W. H. Boom. 1999. Differential regulation of IFN-γ, TNF-α, and IL-10 production by CD4$^+$ $\alpha\beta$TCR$^+$ T cells and Vδ2$^+$ $\gamma\delta$ T cells in response to monocytes infected with *Mycobacterium tuberculosis*-H37Ra. *Cell Immunol.* 194: 12–20.
29. Herold, K. C., J. B. Burton, F. Francois, E. Poumian-Ruiz, M. Glandt, and J. A. Bluestone. 2003. Activation of human T cells by FcR nonbinding anti-CD3 mAb, hOKT3γ1(Ala-Ala). *J. Clin. Invest.* 111: 409–418.
30. Gaston, R. S., M. H. Deierhoi, T. Patterson, E. Prasthofer, B. A. Julian, W. H. Barber, D. A. Laskow, A. G. Diethelm, and J. J. Curtis. 1991. OKT3 first-dose reaction: association with T cell subsets and cytokine release. *Kidney Int.* 39: 141–148.
31. Wagatsuma, M., M. Kimura, R. Suzuki, F. Takeuchi, K. Matsuta, and H. Watanabe. 1996. Ezrin, radixin and moesin are possible auto-immune antigens in rheumatoid arthritis. *Mol. Immunol.* 33: 1171–1176.
32. Kaufman, D. W., J. P. Kelly, M. Levy, and S. Shapiro. 1991. *The Drug Etiology of Agranulocytosis and Aplastic Anemia.* Oxford University Press, New York.
33. Lipsky, P. E., D. M. van der Heijde, E. W. St. Clair, D. E. Furst, F. C. Breedveld, J. R. Kalden, J. S. Smolen, M. Weisman, P. Emery, M. Feldmann, et al. 2000. Infliximab and methotrexate in the treatment of rheumatoid arthritis: anti-tumor necrosis factor trial in rheumatoid arthritis with Concomitant Therapy Study Group. *N. Engl. J. Med.* 343: 1594–1602.
34. Klareskog, L., D. van der Heijde, J. P. de Jager, A. Gough, J. Kalden, M. Malaise, E. Martin Mola, K. Pavelka, J. Sany, L. Settas, et al. 2004. Therapeutic effect of the combination of etanercept and methotrexate compared with each treatment alone in patients with rheumatoid arthritis: double-blind randomized controlled trial. *Lancet* 363: 675–681.
35. Maini, R., E. W. St. Clair, F. Breedveld, D. Furst, J. Kalden, M. Weisman, J. Smolen, P. Emery, G. Harriman, M. Feldmann, and P. Lipsky. 1999. Infliximab (chimeric anti-tumour necrosis factor α monoclonal antibody) versus placebo in rheumatoid arthritis patients receiving concomitant methotrexate: a randomized phase III trial. ATTRACT Study Group. *Lancet* 354: 1932–1939.
36. Deeg, H. J., J. Gotlib, C. Beckham, K. Dugan, L. Holmberg, M. Schubert, F. Appelbaum, and P. Greenberg. 2002. Soluble TNF receptor fusion protein (etanercept) for the treatment of myelodysplastic syndrome: a pilot study. *Leukemia* 16: 162–164.
37. Raza, A., A. Candoni, U. Khan, L. Lisak, S. Tahir, F. Silvestri, J. Billmeier, M. I. Alvi, M. Mumtaz, S. Gezer, P. Venugopal, P. Reddy, and N. Galili. 2004. Remicade as TNF suppressor in patients with myelodysplastic syndromes. *Leuk. Lymphoma* 45: 2099–2104.
38. Hansen, P. B., and A. M. Lauritzen. 2005. Aplastic anemia successfully treated with rituximab. *Am. J. Hematol.* 80: 292–294.
39. Castiglioni, M. G., P. Scatena, C. Pandolfo, S. Mechelli, and M. Bianchi. 2006. Rituximab therapy of severe aplastic anemia induced by fludarabine and cyclophosphamide in a patient affected by B-cell chronic lymphocytic leukemia. *Leuk. Lymphoma* 47: 1985–1986.

Bone Marrow Transplantation (2008) 42, 99–103

www.nature.com/bmt

ORIGINAL ARTICLE

Allo-SCT using reduced-intensity conditioning against advanced pancreatic cancer: a Japanese survey

Y Kanda[1], Y Omuro[2], E Baba[3], K Oshima[1], K Nagafuji[3], Y Heike[4], Y Takaue[4], T Sasaki[2], H Sakamaki[5] and M Harada[3]

[1]*Division of Hematology, Saitama Medical Center, Jichi Medical University, Saitama, Japan;* [2]*Department of Chemotherapy, Tokyo Metropolitan Cancer and Infectious Disease Center, Komagome Hospital, Tokyo, Japan;* [3]*First Department of Internal Medicine, Kyushu University, Fukuoka, Japan;* [4]*Division of Hematology and Stem Cell Transplantation, National Cancer Center Hospital, Tokyo, Japan and* [5]*Hematology Division, Tokyo Metropolitan Cancer and Infectious Disease Center, Komagome Hospital, Tokyo, Japan*

Pancreatic cancer is a frequent cause of cancer-related mortality and has an extremely poor prognosis. To evaluate the efficacy of allogeneic hematopoietic SCT with reduced-intensity conditioning (RICT) against pancreatic cancer, we analyzed the clinical data of 22 patients. After a fludarabine-based conditioning regimen followed by the infusion of PBSCs, all but two achieved engraftment. Complete, partial and minor response was observed in 1, 2 and 2 patients, respectively, with an overall response rate of 23%. Median survival was only 139 days and the major cause of death was tumor progression. Poor performance status before RICT and a lower number of infused CD34-positive cells were associated with shorter survival after RICT. Patients who developed chronic GVHD tended to survive longer than those who did not. These findings support the investigation of a novel treatment strategy to enhance the immunological effect against pancreatic cancer.

Bone Marrow Transplantation (2008) **42**, 99–103;
doi:10.1038/bmt.2008.94; published online 7 April 2008
Keywords: reduced-intensity conditioning; SCT; mini-transplantation; pancreatic cancer; graft-versus-tumor effect

Introduction

Allogeneic hematopoietic SCT is an established treatment for a variety of hematological disorders. However, its application has been limited to young patients because of various complications including regimen-related toxicities, GVHD, infection and so on. Therefore, SCT with reduced-intensity conditioning (RICT) has been investigated for use in older or clinically infirm patients. The antitumor effect of this therapeutic approach depends not only on the antineoplastic agents and/or irradiation in the conditioning regimen, but also on the immunological graft-versus-tumor effect after RICT.[1] Although RICT has not been clearly shown to have a clinical advantage over conventional chemotherapy, some studies have suggested that RICT may be beneficial in elderly patients with hematological malignancies.[2]

Since the late 1990s, several studies of RICT against advanced solid tumors have been performed to harness the graft-versus-tumor effect.[3] A clinical tumor response after RICT was observed in several solid tumors, especially in renal cell cancer and breast cancer.[4–6] Pancreatic cancer is the fifth most common cause of cancer-related mortality in Japan and the United States, and carries an extremely poor prognosis. The median duration of survival in advanced pancreatic cancer is less than 6 months, even when patients are treated with gemcitabine.[7] The combination of gemcitabine with the other chemotherapeutic agents failed to significantly improve survival.[8–10] Furthermore, although the combination of gemcitabine and erlotinib, a molecular targeting agent against epidermal growth factor receptor, significantly prolonged survival, the difference in median survival was only 2 weeks.[11] Because of this poor prognosis by chemotherapy, treatment strategies to enhance immunological effects against pancreatic cancer have been investigated. One of these is a vaccination targeting tumor-specific antigens such as CA19-9 and CEA.[12] Another strategy is RICT to harness a strong allogeneic immunological antitumor effect. The first successful application of RICT against pancreatic cancer was reported in 2001.[13] Several other reports have suggested the existence of an immunological graft-versus-tumor effect against pancreatic cancer, but the number of patients in each report was too small to draw any meaningful conclusion.[14,15] Therefore, we collected the clinical results of RICT against pancreatic cancer from transplantation centers in Japan, in which a prospective clinical trial of RICT against pancreatic cancer had been performed.

Correspondence: Dr Y Kanda, Division of Hematology, Saitama Medical Center, Jichi Medical University, 1-847 Amanuma, Omiya-ku, Saitama City, Saitama 330-8503, Japan.
E-mail: ycanda-tky@umin.ac.jp
Received 28 January 2008; revised 28 February 2008; accepted 5 March 2008; published online 7 April 2008

Patients and methods

We surveyed transplantation centers in Japan and identified three centers (Komagome Hospital, Kyushu University and National Cancer Center Hospital) that were performing a prospective clinical trial against various advanced solid tumors including pancreatic cancer. The University of Tokyo Hospital was performing a trial that exclusively included patients with advanced pancreatic cancer. Two of these trials have already been published.[14,15] We collected the clinical results of all patients with pancreatic cancer who participated in these studies from the published papers or using a questionnaire.

The reduced-intensity conditioning regimens were exclusively fludarabine-based, but varied among centers. The most intensive regimen was the combination of fludarabine (30 mg/m^2/day for 6 days), BU (4 mg/kg/day for 2 days) and gemcitabine (1000 mg/m^2/day for 3 days) at the University of Tokyo Hospital, whereas the combination of fludarabine (30 mg/m^2/day for 3 days) and TBI at 2 Gy (Kyushu University) was the least intensive. CY (60 mg/kg/day for 2 days) was combined with fludarabine (25 mg/m^2/day for 5 days) in the Komagome Hospital. Prophylaxis against GVHD was performed with CYA either alone or in combination with MTX or mycophenolate mofetil. PBSCs were mobilized with G-CSF, cryopreserved using standard techniques without *ex vivo* manipulation, thawed and infused on day 0. Host/donor T-cell chimerism was analyzed by sex-chromosome FISH or the short tandem repeat method after transplantation.[16]

The tumor response to treatment was evaluated as described previously.[15] Briefly, CR (complete response) was defined as disappearance of all clinical evidence of tumor for a minimum of 4 weeks by computed tomography scan. MR (minor response) and PR (partial response) were defined as decreases of 25–50% and greater than 50%, respectively, in the sum of the products of the maximum diameter and its perpendicular diameter of all measurable lesions for a minimum of 4 weeks.[7]

Engraftment was defined as a neutrophil count more than 500/mm^3 for 3 consecutive days after RICT. Engraftment failure was diagnosed as when engraftment was not achieved at any time after transplantation. The probability of survival was calculated using the Kaplan–Meier method. The incidence of chronic GVHD was evaluated in 13 patients who survived longer than 100 days after RICT. Univariate comparisons for dichotomous and time-to-event variables between groups were performed with the Fisher exact test and the log-rank test, respectively, and multivariate analyses were performed using logistic regression analysis and proportional hazards modeling, respectively. Factors associated with at least borderline significance ($P<0.10$) in the univariate analysis were subjected to a multivariate analysis using backward stepwise selection of covariates. All P-values were two sided and values of 0.05 or less were considered statistically significant.

Results

Clinical data of 22 patients with a median age of 57 years (range: 36–68 years) were collected (Table 1). There were 15 male and seven female patients. Fifteen patients had metastatic disease, whereas 7 had locally advanced diseases. All but one patient had received chemotherapy with gemcitabine either alone or in combination with other antineoplastic agents before RICT. In all, 10 had received local irradiation in addition to chemotherapy. Eastern Cooperative Oncology Group performance status (ECOG-PS) was equal to or greater than 2 in 10 patients. The conditioning regimen was fludarabine-BU-based in 10, fludarabine-CY in 7 and fludarabine-TBI in 5. The donors were HLA-matched relatives except in one patient who received graft from an HLA-mismatched family donor. The number of CD34-positive cells infused was greater than 4.0×10^6 cells/recipient body weight (kg) in 10 patients. CYA was used for GVHD prophylaxis: alone in 8, combined with MTX in 10 and combined with mycophenolate mofetil in 4.

Engraftment was observed in all but two patients with a median duration from RICT of 12 days (range: 6–42 days). Complete donor-type T-cell chimerism was confirmed in 18 patients, whereas mixed chimerism persisted in 4 patients. A total of 12 patients developed grade II–IV acute GVHD. Limited and extensive chronic GVHD was observed in three and five patients, respectively, among the 13 patients who survived longer than 100 days after RICT.

The best response after RICT was CR in one, PR in two, MR in two and stable disease in eight. The overall response

Table 1 Characteristics of the patients

Age (years)	
Median	57
Range	36–68
Sex	
Male	15
Female	7
Disease	
Locally advanced	7
Metastatic	15
ECOG-PS	
0–1	12
2–4	10
Regimen	
Flu + BU + Gem	7
Flu + CY	6
Flu + TBI	6
Flu + BU	3
Donor	
HLA-matched sibling	21
Mismatched family donor	1
CD34+ cells in graft	
$\leq 4.0 \times 10^6$/kg	12
$> 4.0 \times 10^6$/kg	10
GVHD prophylaxis	
CsA alone	8
CsA + MTX	10
CsA + MMF	4

Abbreviations: ECOG-PS = Eastern Cooperative Oncology Group performance status; Flu = fludarabine; Gem = gemcitabine; MMF = mycophenolate mofetil.

rate (CR + PR + MR) was 23%. A univariate analysis to identify possible relationships between clinical parameters and overall response failed to show any statistically significant factors. The conditioning regimen did not significantly affect the response rate, although the statistical power was not enough due to the small number of patients in each group. Response was observed in two of the seven patients who received the most intensive regimen including fludarabine, BU and gemcitabine, while it was seen in one of the six patients who received the least intensive regimen with fludarabine and low-dose TBI. None of the patients with mixed chimerism showed a response, but this difference was not statistically significant. DLI (donor lymphocyte infusion) was performed in four patients who had progressive disease after RICT, and the number of infused CD3-positive cells was between 2.7×10^7 and 1.8×10^8 cells/kg. One patient showed tumor shrinkage after DLI, but the response was transient.

Figure 1a shows overall survival after RICT. Median survival was only 139 days and the major cause of death was tumor progression. Other causes of death included infection in one and chronic GVHD in two. In a univariate analysis, ECOG-PS below 2 and infused CD34-positive cell dose greater than 4.0×10^6 cells/kg were associated with significantly longer survival after RICT (Table 2; Figures 1b and c). A multivariate analysis revealed that these two factors were almost independently significant (Table 2). With regard to post transplantation factors, while the development of grade II–IV acute GVHD did not significantly affect survival ($P = 0.76$), the eight patients who developed chronic GVHD tended to survive longer than those who survived longer than 100 days after RICT but did not develop chronic GVHD ($P = 0.092$; Figure 2). This analysis was unlikely to be biased by the fact that patients who survived longer had more chance to develop chronic GVHD, as most of the patients developed chronic GVHD as a progressive type from acute GVHD.

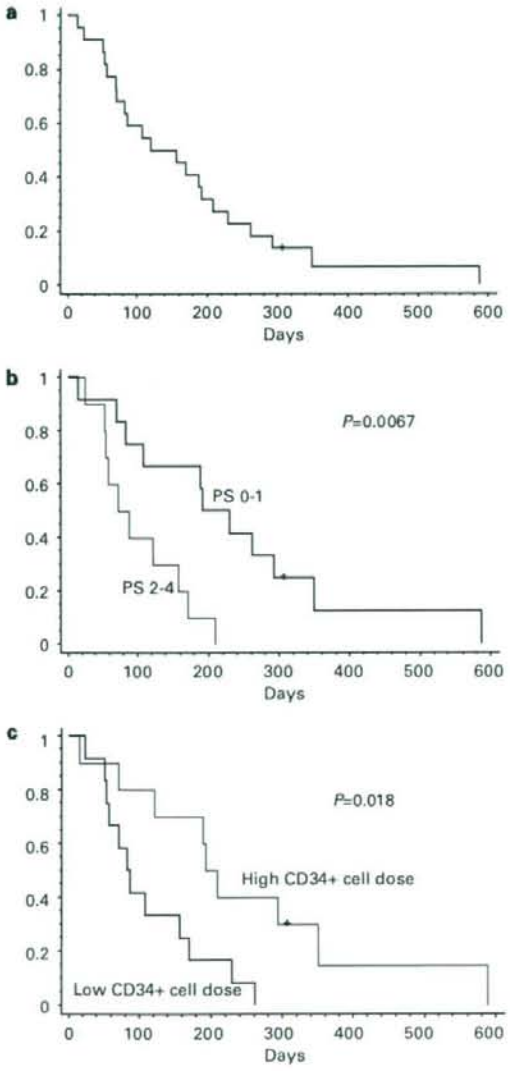

Figure 1 Patient survival, overall (**a**) and grouped according to risk factors (**b** and **c**).

Discussion

To summarize these findings, 23% of the 22 patients in this series showed a response to RICT. However, the duration of the response was generally short and most of the patients eventually died with progressive disease. The median survival after RICT was only 139 days and only one survived longer than 1 year after transplantation. Good ECOG-PS and higher number of CD34-positive cells in the graft were independently associated with longer survival.

The relationship between the number of infused CD34-positive cells and transplant outcome has been studied in PBSC transplantation for hematological malignancies.[17] The infusion of a higher number of CD34-positive cells has been associated with faster recovery of neutrophils and plts, but chronic GVHD was more frequently observed in patients who received a very high dose of CD34-positive cells (that is, $>8.0 \times 10^6$ cells/kg). In this study, two patients failed to achieve engraftment, and both had received less than 4.0×10^6 cells/kg of CD34-positive cells. However, a statistically significant survival advantage was confirmed even after these two patients were excluded from the analysis. If we consider that the major cause of death in this study was progressive disease, the infusion of a higher number of CD34-positive cells might have protected patients from disease progression by a graft-versus-host reaction, although we failed to show a significant difference between the number of infused CD34-positive cells and tumor response or the incidence of chronic GVHD, probably due to the small number of patients. Patients who developed chronic GVHD showed better survival than those who did not, with a borderline significance, suggesting that they had some immunological protection against the progression of pancreatic cancer.

Table 2 Univariate and multivariate analyses for overall survival

Factor	*Median survival (days)*	*P-value*
A. Univariate		
Age (years)		
<55	115	0.63
≥55	180	
Sex		
Male	87	0.69
Female	170	
ECOG-PS		
0–1	211	0.0067
2–4	80	
Stage		
Locally advanced	192	0.21
Metastatic	121	
Serum CEA		
Negative	122	0.70
Positive	192	
Serum CA19-9		
Negative	157	0.84
Positive	132	
Regimen		
Flu + BU based	191	0.25
Flu + CY	156	
Flu + TBI	71	
CD34+ cell dose		
$\leq 4.0 \times 10^6$/kg	85	0.018
$>4.0 \times 10^6$/kg	201	
GVHD prophylaxis		
CsA alone	132	0.55
CsA + MTX	191	
CsA + MMF	96	
B. Multivariate	*Relative risk (95% CI)*	*P-value*
ECOG-PS		
0–1	1.00	0.032
2–4	3.39 (1.11–10.3)	
CD34+ cell dose		
$\leq 4.0 \times 10^6$/kg	1.00	0.068
$>4.0 \times 10^6$/kg	0.37 (0.13–1.07)	

Abbreviations: CI = confidence interval; ECOG-PS = Eastern Cooperative Oncology Group performance status; Flu = fludarabine; MMF = mycophenolate mofetil.

This study was limited by the heterogeneity of transplantation procedures among centers. However, considering the difficulty of performing a large-scale prospective study on RICT against pancreatic cancer, this small survey may currently represent the best evidence of the efficacy of this novel treatment strategy against advanced pancreatic cancer and may suggest a future direction for improving the treatment outcome. We showed that pancreatic cancer can be a possible target for allogeneic immunotherapy. However, the immunological effect was not strong or durable enough to prevent tumor progression. A possible strategy for enhancing a graft-versus-tumor effect against pancreatic cancer without enhancing GVHD is a combination with specific immunotherapy using antigens including CA19-9,

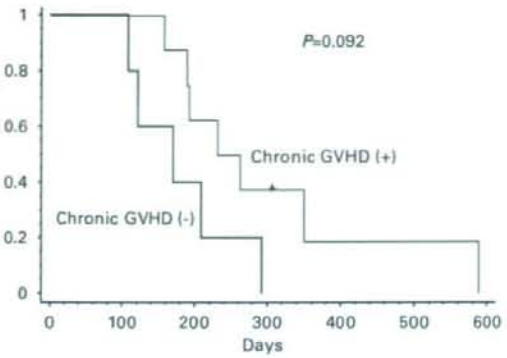

Figure 2 Overall survival of patients who survived at least 100 days after transplantation grouped according to the presence or absence of chronic GVHD.

CA242, CEA, Her-2, mutated K-ras and MUC-1.[12] Among these, CEA is attractive, since it is expressed in 85–90% of pancreatic cancer, and a specific immunotherapy against CEA could also be applied to other gastrointestinal cancers. An increase in the serum anti-CEA antibody level associated with a tumor response was observed in the University of Tokyo Study.[15] In addition, Kim *et al.*[18] showed that a peptide CEA652, TYACFVSNL, binds to HLA-A24 and induces CEA-specific cytotoxic T cells. Therefore, vaccination with such a peptide may be promising as a post transplantation immunotherapy against pancreatic cancer. Another approach is to add molecular targeting agents such as erlotinib after RICT. This may induce tumor cell death, leading to the enhanced presentation of tumor antigens to donor T cells. In addition, RICT can be combined with surgical resection, since the prognosis of pancreatic cancer is very poor even after complete resection.[19,20] Maximum graft-versus-tumor effect can be expected when the tumor load is at its lowest level.

In conclusion, a tumor response was observed in approximately one-fourth of the patients who underwent RICT against advanced pancreatic cancer. Although the response was not durable, our findings, such as the relationship between longer survival and the infusion of a higher number of CD34-positive cells or the development of chronic GVHD, should support a future study to enhance the specific immunological effect against pancreatic cancer.

References

1 Champlin R, Khouri I, Shimoni A, Gajewski J, Kornblau S, Molldrem J *et al.* Harnessing graft-versus-malignancy: non-myeloablative preparative regimens for allogeneic haematopoietic transplantation, an evolving strategy for adoptive immunotherapy. *Br J Haematol* 2000; **111**: 18–29.

2 Mohty M, de Lavallade H, Ladaique P, Faucher C, Vey N, Coso D *et al.* The role of reduced intensity conditioning allogeneic stem cell transplantation in patients with acute myeloid leukemia: a donor vs no donor comparison. *Leukemia* 2005; **19**: 916–920.

3 Bregni M, Ueno NT, Childs R. The second international meeting on allogeneic transplantation in solid tumors. *Bone Marrow Transplant* 2006; **38**: 527–537.
4 Ueno NT, Cheng YC, Rondon G, Tannir NM, Gajewski JL, Couriel DR *et al.* Rapid induction of complete donor chimerism by the use of a reduced-intensity conditioning regimen composed of fludarabine and melphalan in allogeneic stem cell transplantation for metastatic solid tumors. *Blood* 2003; **102**: 3829–3836.
5 Bregni M, Dodero A, Peccatori J, Pescarollo A, Bernardi M, Sassi I *et al.* Nonmyeloablative conditioning followed by hematopoietic cell allografting and donor lymphocyte infusions for patients with metastatic renal and breast cancer. *Blood* 2002; **99**: 4234–4236.
6 Childs R, Chernoff A, Contentin N, Bahceci E, Schrump D, Leitman S *et al.* Regression of metastatic renal-cell carcinoma after nonmyeloablative allogeneic peripheral-blood stem-cell transplantation. *N Engl J Med* 2000; **343**: 750–758.
7 Burris III HA, Moore MJ, Andersen J, Green MR, Rothenberg ML, Modiano MR *et al.* Improvements in survival and clinical benefit with gemcitabine as first-line therapy for patients with advanced pancreas cancer: a randomized trial. *J Clin Oncol* 1997; **15**: 2403–2413.
8 Herrmann R, Bodoky G, Ruhstaller T, Glimelius B, Bajetta E, Schuller J *et al.* Gemcitabine plus capecitabine compared with gemcitabine alone in advanced pancreatic cancer: a randomized, multicenter, phase III trial of the Swiss Group for Clinical Cancer Research and the Central European Cooperative Oncology Group. *J Clin Oncol* 2007; **25**: 2212–2217.
9 Berlin JD, Catalano P, Thomas JP, Kugler JW, Haller DG, Benson III AB. Phase III study of gemcitabine in combination with fluorouracil versus gemcitabine alone in patients with advanced pancreatic carcinoma: Eastern Cooperative Oncology Group Trial E2297. *J Clin Oncol* 2002; **20**: 3270–3275.
10 Heinemann V, Quietzsch D, Gieseler F, Gonnermann M, Schonekas H, Rost A *et al.* Randomized phase III trial of gemcitabine plus cisplatin compared with gemcitabine alone in advanced pancreatic cancer. *J Clin Oncol* 2006; **24**: 3946–3952.
11 Moore MJ, Goldstein D, Hamm J, Figer A, Hecht JR, Gallinger S *et al.* Erlotinib plus gemcitabine compared with gemcitabine alone in patients with advanced pancreatic cancer: a phase III trial of the National Cancer Institute of Canada Clinical Trials Group. *J Clin Oncol* 2007; **25**: 1960–1966.
12 Kaufman HL, Di Vito Jr J, Horig H. Immunotherapy for pancreatic cancer: current concepts. *Hematol Oncol Clin North Am* 2002; **16**: 159–197, viii.
13 Omuro Y, Matsumoto G, Sasaki T, Tanaka Y, Maeda Y, Sakamaki H *et al.* Regression of an unresectable pancreatic tumor following nonmyeloablative allogeneic peripheral-blood stem-cell transplantation. *Bone Marrow Transplant* 2003; **31**: 943–945.
14 Takahashi T, Omuro Y, Matsumoto G, Sakamaki H, Maeda Y, Hiruma K *et al.* Nonmyeloablative allogeneic stem cell transplantation for patients with unresectable pancreatic cancer. *Pancreas* 2004; **28**: e65–e69.
15 Kanda Y, Komatsu Y, Akahane M, Kojima S, Asano-Mori Y, Tada M *et al.* Graft-versus-tumor effect against advanced pancreatic cancer after allogeneic reduced-intensity stem cell transplantation. *Transplantation* 2005; **79**: 821–827.
16 Thiede C, Florek M, Bornhauser M, Ritter M, Mohr B, Brendel C *et al.* Rapid quantification of mixed chimerism using multiplex amplification of short tandem repeat markers and fluorescence detection. *Bone Marrow Transplant* 1999; **23**: 1055–1060.
17 Heimfeld S. HLA-identical stem cell transplantation: is there an optimal CD34 cell dose? *Bone Marrow Transplant* 2003; **31**: 839–845.
18 Kim C, Matsumura M, Saijo K, Ohno T. *In vitro* induction of HLA-A2402-restricted and carcinoembryonic-antigen-specific cytotoxic T lymphocytes on fixed autologous peripheral blood cells. *Cancer Immunol Immunother* 1998; **47**: 90–96.
19 Trede M, Schwall G, Saeger HD. Survival after pancreatoduodenectomy. 118 consecutive resections without an operative mortality. *Ann Surg* 1990; **211**: 447–458.
20 Geer RJ, Brennan MF. Prognostic indicators for survival after resection of pancreatic adenocarcinoma. *Am J Surg* 1993; **165**: 68–72; discussion 72–63.

Human Flt3 Is Expressed at the Hematopoietic Stem Cell and the Granulocyte/Macrophage Progenitor Stages to Maintain Cell Survival[1]

Yoshikane Kikushige,*† Goichi Yoshimoto,*† Toshihiro Miyamoto,† Tadafumi Iino,†§ Yasuo Mori,*† Hiromi Iwasaki,† Hiroaki Niiro,† Katsuto Takenaka,* Koji Nagafuji,* Mine Harada,* Fumihiko Ishikawa,‡ and Koichi Akashi[2]*†§

FLT3/FLK2, a member of the receptor tyrosine kinase family, plays a critical role in maintenance of hematopoietic homeostasis, and the constitutively active form of the FLT3 mutation is one of the most common genetic abnormalities in acute myelogenous leukemia. In murine hematopoiesis, Flt3 is not expressed in self-renewing hematopoietic stem cells, but its expression is restricted to the multipotent and the lymphoid progenitor stages at which cells are incapable of self-renewal. We extensively analyzed the expression of Flt3 in human (h) hematopoiesis. Strikingly, in both the bone marrow and the cord blood, the human hematopoietic stem cell population capable of long-term reconstitution in xenogeneic hosts uniformly expressed Flt3. Furthermore, human Flt3 is expressed not only in early lymphoid progenitors, but also in progenitors continuously along the granulocyte/macrophage pathway, including the common myeloid progenitor and the granulocyte/macrophage progenitor. We further found that human Flt3 signaling prevents stem and progenitors from spontaneous apoptotic cell death at least through up-regulating Mcl-1, an indispensable survival factor for hematopoiesis. Thus, the distribution of Flt3 expression is considerably different in human and mouse hematopoiesis, and human FLT3 signaling might play an important role in cell survival, especially at stem and progenitor cells that are critical cellular targets for acute myelogenous leukemia transformation. *The Journal of Immunology*, 2008, 180: 7358–7367.

Hematopoiesis is one of the most intensely studied stem cell systems where hematopoietic stem cells (HSCs)[3] self-renew, generate a variety of lineage-restricted progenitors, and continuously supply all types of mature blood cells. The technical advances of the multicolor FACS and the use of mAbs have enabled the prospective isolation of hematopoietic stem and progenitor cells according to the surface marker expression. In mice, multipotent hematopoietic activity resides in a small fraction of bone marrow (BM) cells lacking the expression of lineage-associated surface marker (Lin) but expressing high levels of Sca-1 and c-Kit (1, 2). Within the c-Kit$^+$Lin$^-$Sca-1$^+$ (KLS) fraction, the most primitive self-renewing HSCs with long-term reconstituting activity (LT-HSCs) do not express murine (m) CD34, but they do express mCD38 and a low level of mCD90 (Thy1), whereas mCD34$^+$, mCD38$^-$, or mThy1$^-$ KLS cells are short-term HSCs (ST-HSCs) or multipotent progenitors that do not self-renew (3–5). Downstream of the mCD34$^+$ ST-HSC stage, common lymphoid progenitors (CLPs) (6) and common myeloid progenitors (CMPs) (7) that can differentiate into all lymphoid cells and myelo-erythroid cells, respectively, have been purified. CMPs differentiate into granulocyte/macrophage progenitors (GMPs) and megakaryocyte/erythrocyte progenitors (MEPs), both of which are also prospectively isolatable by FACS (7).

Interestingly, the expression pattern of these surface markers in early stem and progenitor populations are considerably different in human (h) hematopoiesis. In humans, LT-HSCs express hCD34 (8). The hLT-HSC resides in the hCD34$^+$hCD38$^-$ (9, 10) or the hCD34$^+$hCD90$^+$ (11–13) fractions in both human BM and cord blood (CB). It is still unclear what percent of hCD34$^+$hCD38$^-$ or hCD34$^+$hCD90$^+$ cells are LT-HSCs in human hematopoiesis. The human counterpart for mCMPs, mGMPs, mMEPs, or mCLPs is also isolatable in the BM and the CB within the hCD34$^+$hCD38$^+$ progenitor fraction (14, 15). It has thus been suggested that, despite the difference in the expression patterns of key Ags in human and mouse hematopoiesis, lineage commitment processes from HSCs to mature blood cells might be generally preserved in both species. For example, the existence of prospectively isolatable CMPs and CLPs suggests that lineage commitment from HSCs involves myeloid vs lymphoid bifurcation in both mouse and human.

Recently, two independent groups have reported that in murine hematopoiesis, Flt3/Flk2, a tyrosine kinase receptor, is expressed in ST-HSCs but not in LT-HSCs. One group showed that mCD34$^-$

*Medicine and Biosystemic Science, and †Center for Cellular and Molecular Medicine, Kyushu University Graduate School of Medical Sciences, Fukuoka, and ‡Research Unit for Human Disease Model, RIKEN Center for Allergy and Immunology, Kanagawa, Japan; and §Department of Cancer Immunology and AIDS Dana-Farber Cancer Institute, Harvard Medical School, Boston, MA 02115

Received for publication November 26, 2007. Accepted for publication March 25, 2008.

The costs of publication of this article were defrayed in part by the payment of page charges. This article must therefore be hereby marked *advertisement* in accordance with 18 U.S.C. Section 1734 solely to indicate this fact.

[1] This work was supported in part by a Grant-in-Aid from the Ministry of Education, Culture, Sports, Science and Technology in Japan (19659248 to T.M., and 17109010 and 17047029 to K.A.) and the Mochida Memorial Foundation for Medical and Pharmaceutical Research (to T.M.).

[2] Address correspondence and reprint requests to Dr. Koichi Akashi, Medicine and Biosystemic Science, Kyushu University Graduate School of Medical Sciences, 3-1-1 Maidashi, Higashi-ku, Fukuoka, Japan. E-mail address: akashi@med.kyushu-u.ac.jp

[3] Abbreviations used in this paper: HSC, hematopoietic stem cell; AML, acute myelogenous leukemia; BM, bone marrow; KLS, c-Kit$^+$Lin$^-$Sca-1$^+$; LT-HSC, HSC with long-term reconstituting activity; ST-HSC, short-term HCS; m, murine; h, human; CLP, common lymphoid progenitor; CMP, common myeloid progenitor; GM, granulocyte/macrophage; GMP, GM progenitor; MEP, megakaryocyte/erythrocyte progenitor; CB, cord blood; MegE, megakaryocyte/erythrocyte; FL, Flt3 ligand; PI, propidium iodide; SCF, stem cell factor; Tpo, thrombopoietin; Epo, erythropoietin; CFU-GEMM, CFU-granulocyte/erythroid/macrophage/megakaryocyte; RTK, receptor tyrosine kinase; ITD, internal tandem duplication.

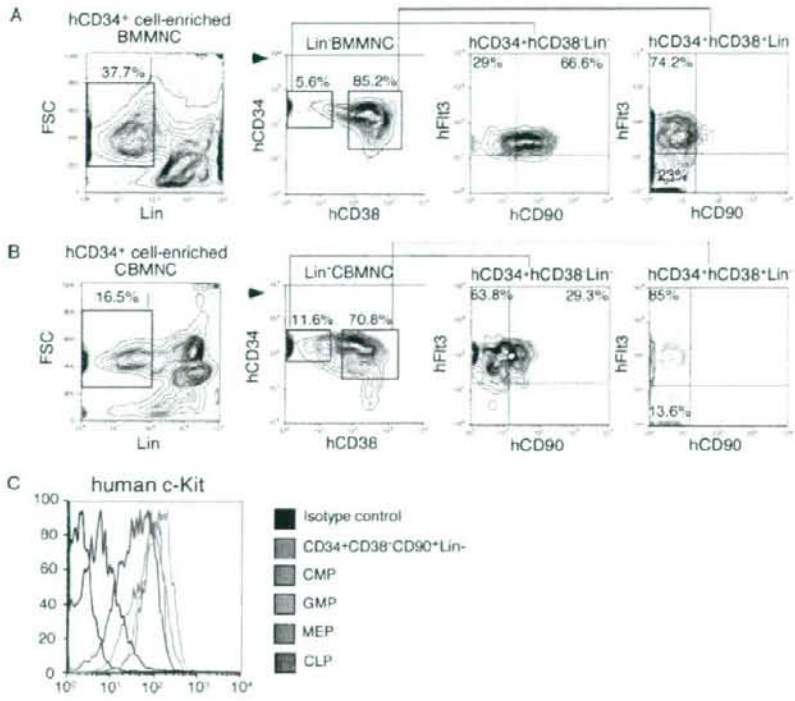

FIGURE 1. A flow cytometric analyses of human early hematopoietic populations in the BM and the CB. In hCD34$^+$hCD38$^-$ immature BM (*A*) and CB (*B*) cells, hFlt3 was expressed at a low level in both hCD90 (Thy1) positive and negative fractions. In contrast, the hCD34$^+$hCD38$^+$ BM and CB progenitor populations did not express hCD90, and hFlt3 was expressed in only a fraction of these populations. *C*, hHSCs and myeloid progenitors expressed c-Kit at high levels, and CLPs at a low level. Representative data of independent five experiments are shown here.

KLS cells (LT-HSCs) are mFlt3$^-$ (16), and the other showed that only the mFlt3$^-$ fraction of mCD90^{low} KLS cells possesses LT-HSC activity (17). Each group further studied the detailed differentiation activity of mFlt3$^+$ KLS cells, but drew different conclusions. Adolfsson et al. (18) reported that the mFlt3$^+$mCD34$^+$ KLS population maintains the granulocyte/macrophage (GM) and the T/B lymphoid, but not the megakaryocyte/erythrocyte (MegE) potential, if any. This result suggests that, in addition to the lymphoid vs myeloid developmental pathway represented by CLPs and CMPs, respectively, there is a critical stage common to GM, T, and B lymphoid cells. The other group, however, showed that mFlt3$^+$mCD90$^-$ KLS cells are multipotent, thus claiming that the stage common to GM/lymphoid lineages proposed by Adolfsson et al. (18) does not constitute a major pathway for hematopoietic development (19). In contrast, downstream of the mST-HSC stage, there is a general agreement that mFlt3 is expressed in progenitors with lymphoid potential, such as the majority of CLPs and a minor fraction of CMPs, that retain a weak B cell potential (20), whereas it is down-regulated in late myeloid stages, such as GMPs and MEPs (20, 21). The Flt3 ligand (FL) is required for development of CLPs from mFlt3$^+$ KLS cells, whereas mFlt3 is dispensable for HSC maintenance and myeloid development (22). These results suggest that in mouse hematopoiesis, Flt3 signaling plays an important role in lymphoid, but not in HSC or myeloid, development.

The precise expression and the role of hFlt3 in human hematopoiesis, however, remain unclear. Around 40–80% of hCD34$^+$ BM and CB cells express hFlt3 (23, 24). Although a fraction of both the hFlt3$^+$ and the hFlt3$^-$ populations gave rise to multilineage "mixed" colonies containing all myelo-erythroid components, the hFlt3$^+$hCD34$^+$ and hFlt3$^-$hCD34$^+$ populations predominantly formed GM and erythroid colonies, respectively (23–25). It has also been shown that cells with NOD/SCID reconstitution activity reside in the hCD34$^+$hFlt3$^+$ fraction (24). These data collectively suggest that LT-HSCs and GMPs may reside mainly in the hFlt3$^+$hCD34$^+$ fraction, whereas MEPs may be contained in the hFlt3$^-$hCD34$^+$ fraction. Therefore, the expression pattern of Flt3 could be quite different in mouse and human hematopoiesis. Flt3 expression has also been implicated in development of human acute myelogeneous leukemia (AML). Flt3 is expressed in leukemic blasts in most cases with AML (26, 27). Furthermore, *FLT3* is one of the most frequently mutated genes in AML (28, 29), and the FLT3 mutants transduce the constitutively active FLT3 signaling, that could be the cause of poor prognosis in AML with *FLT3* mutations (30–32).

In this study, we extensively analyzed the expression and function of hFlt3 in steady-state human BM and CB hematopoiesis. Interestingly, hFlt3 was expressed in the entire human BM and CB HSC population, and purified hFlt3$^+$ HSCs could reconstitute multilineage cells for a long-term in our xenogeneic transplantation system (33). Therefore, unlike mouse hematopoiesis, the negative expression of Flt3 does not mark LT-HSCs in human. Furthermore, in striking contrast to mouse hematopoiesis where mFlt3 is expressed in CLPs but not GMPs (20, 21), hFlt3 was expressed in GMPs as well as in CLPs at a high level. The hFlt3 signaling did not affect the lineage fate decision of hHSCs, but supported cell survival of hFlt3$^+$ stem and progenitor cells, at least through the up-regulation of Mcl-1, a survival promoting Bcl-2 homologue (34). These data collectively suggest that Flt3 signaling plays a critical role in maintenance of self-renewing LT-HSCs, and of GM and lymphoid progenitors in human hematopoiesis.

Materials and Methods

BM and CB samples

Fresh human steady-state BM and CB samples were collected from healthy adults and newborns after normal deliveries. Informed consent was obtained from all subjects. The Institutional Review Board of each institution participating in this project approved all research on human subjects.

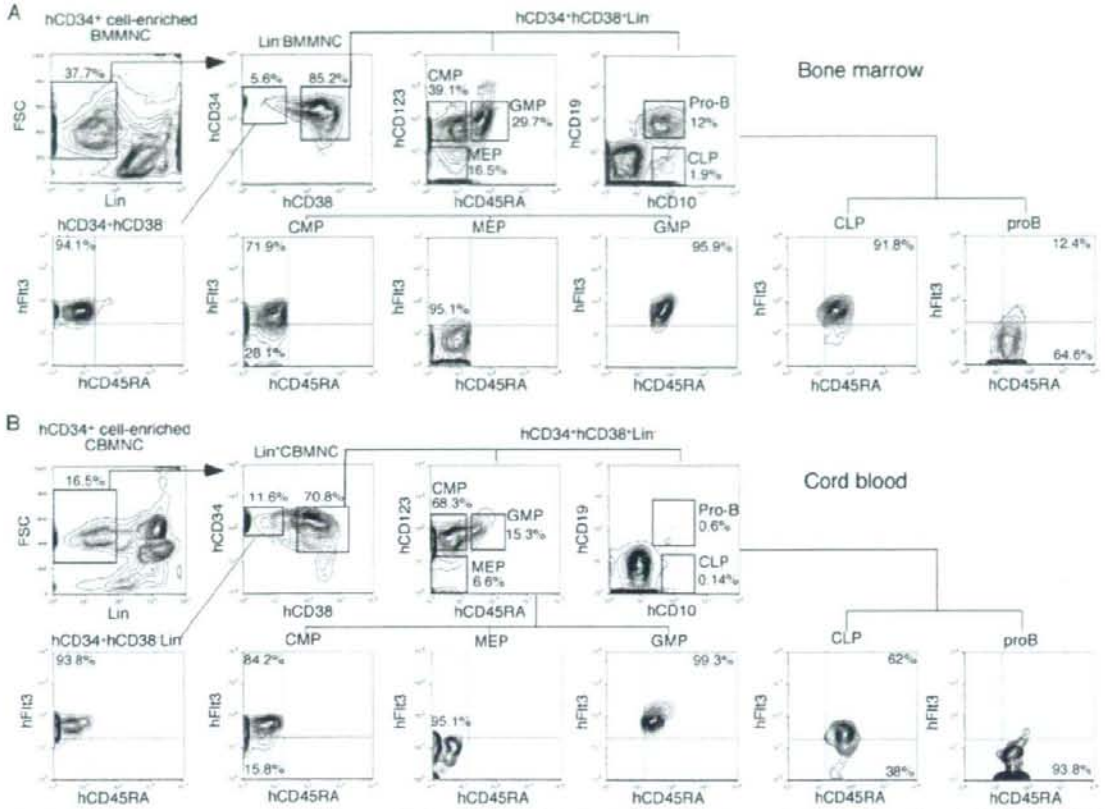

FIGURE 2. The expression patterns of hFlt3 are similar in early human BM (*A*) and CB (*B*) hematopoiesis. In the myeloid pathway in both the BM and CB, hFlt3 was up-regulated into the GM pathway, but was down-regulated in the MegE pathway; GMPs expressed hFlt3 at a high level, whereas MEPs did not express hFlt3. CMPs contained both $hFlt3^+$ and $hFlt3^-$ fractions. In the lymphoid pathway, CLPs expressed hFlt3 at a high level in BM (*A*) and a low level in CB (*B*), whereas $hCD10^+hCD19^+$ proB cells did not express hFlt3 in either the BM or the CB. Representative data of independent five experiments are shown here.

Cell preparation, flow cytometric analysis, and cell sorting

The BM and CB mononuclear cells were prepared by gradient centrifugation and the $CD34^+$ cells were enriched from mononuclear cells by using the Indirect CD34 MicroBead kit (Miltenyi Biotec) as described previously (14). For the analyses and sorting of myeloid progenitors, cells were stained with a Cy5-PE- or PC5-conjugated lineage mixture, including anti-hCD3 (HIT3a), hCD4 (RPA-T4), hCD7, hCD8 (RPA-T8), hCD10 (HI10a), hCD19 (HIB19), hCD20 (2H7), hCD11b (ICFR44), hCD14 (RMO52), hCD56 (NKH-1), and hGPA (GA-R2), FITC-conjugated anti-hCD34 (8G12), or anti-hCD45RA (HI100), PE-conjugated anti-hFlt3 (CD135) (4G8), or anti-hCD123 (6H6), allophycocyanin-conjugated anti-hCD34 (8G12), or anti-hCD38 (HIT2), Pacific Blue-conjugated anti-hCD45RA (HI100), and biotinylated anti-hCD38 (HIT2), or anti-hCD123 (9F5). The lymphoid progenitors were stained with the same lineage mixture except for the omission of anti-hCD10 and hCD19 followed by FITC-conjugated anti-hCD10 (SS2/36), PE-Cy7-conjugated anti-hCD19 (SJ25C1), and anti-hFlt3, hCD34, hCD38, and hCD45RA as described above. For additional analyses, PE-Cy7-conjugated anti-hCD34 (8G12), FITC-conjugated anti-hCD90 (5E10), PE-conjugated anti- hCD117 (YB5.B8), biotinylated anti-hFlt3 (BV10A4H2), and PE-conjugated anti-hCD127 (R34.34) mAbs were used. Streptavidin-conjugated allophycocyanin-Cy7 or PE-Cy7 was used for visualization of the biotinylated Abs (BD Pharmingen). The dead cells were excluded by propidium iodide (PI) staining. Appropriate isotype-matched, irrelevant control mAbs were used to determine the level of background staining. The cells were sorted and analyzed by FACS Aria (BD Biosciences). The sorted cells were subjected to an additional round of sorting using the same gate to eliminate contaminating cells and doublets. For single-cell assays, the re-sort was performed by using an automatic cell-deposition unit system (BD Biosciences).

In vitro assays to determine the differentiation potential of progenitors

Clonogenic CFU assays were performed using a methylcellulose culture system that was set up to detect all possible outcomes of myeloid differentiation as reported previously (14, 35). For myeloid colony formation, cells were cultured in IMDM-based methylcellulose medium (Methocult H4100; StemCell Technologies) supplemented with 20% FCS, 1% BSA, 2 mM L-glutamine, 50 μM 2-ME, and antibiotics in the presence of human cytokines such as IL-3 (20 ng/ml), stem cell factor (SCF) (20 ng/ml), FL (20 ng/ml), IL-11 (10 ng/ml), thrombopoietin (Tpo) (50 ng/ml), erythropoietin (Epo) (4 U/ml), and GM-CSF (50 ng/ml). All cytokines were obtained from R&D Systems. Colony numbers were enumerated on day 14 of culture. For the short-term liquid cell culture, cells were cultured in IMDM with 10% FCS in the presence of the cytokines described above. All of the cultures were incubated at 37°C in a humidified chamber under 5% CO_2.

Apoptosis assay and cytokine stimulation assays in the serum-free medium

To exclude the unexpected effects of FCS and to evaluate the effects of cytokine stimulation precisely, the cells were prepared in the FCS-free condition. The anti-apoptotic effect of FL and SCF was evaluated after 24 h

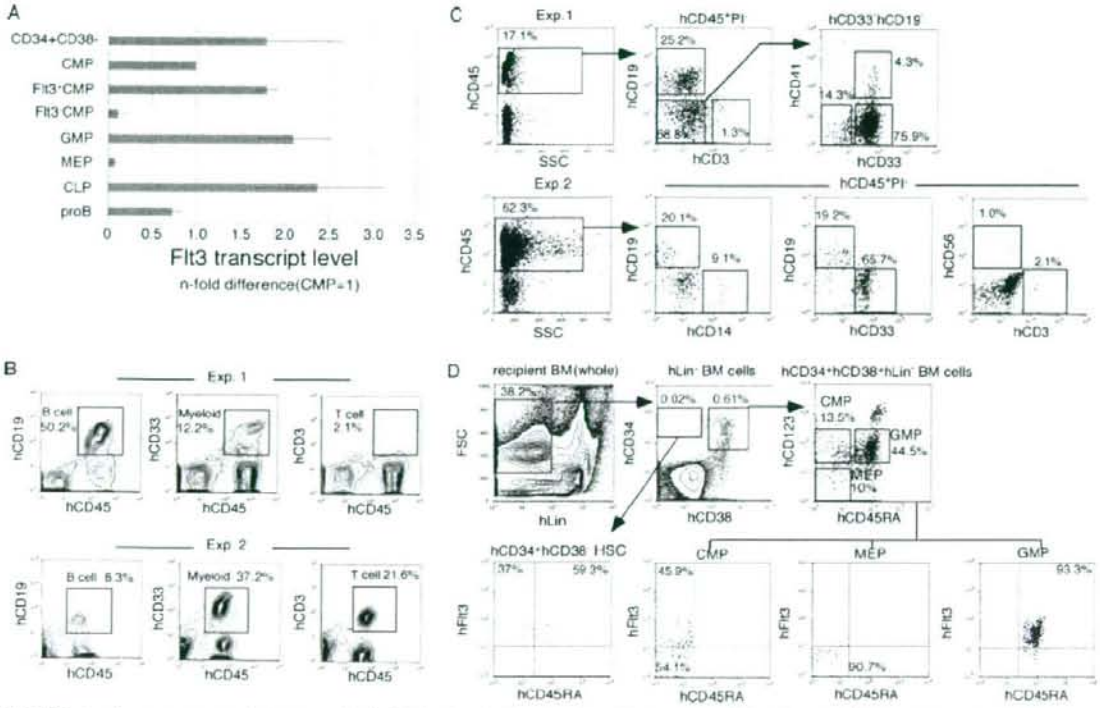

FIGURE 3. Long-term reconstitution potential of hFlt3$^+$hCD34$^+$hCD38$^-$hCD90$^+$Lin$^-$ cells in NOD/SCID/IL2rγ^{null} newborn mice. *A*, Analyses of the relative expression levels of hFlt3 transcript by real-time PCR. Each bar shows the *n*-fold difference of the level of hFlt3 mRNA in comparison to that of the whole CMP. The mean value and SD of BM samples from three independent normal donors are shown. Note that the levels of hFlt3 transcripts are well correlated with those of surface hFlt3 expression determined by FACS (Fig. 2*A*). *B*, The long-term and multilineage reconstitution of human cells in mice injected with 1×10^3 hFlt3$^+$hCD34$^+$hCD38$^-$Lin$^-$ CB cells 4 (*upper panels*) or 6 (*lower panels*) mo after transplantation. Representative two results out of five experiments are shown. *C*, Multilineage reconstitution 6 (*upper panels*) and 15 wk (*lower panels*) after i.v. injection of 5×10^3 hFlt3$^+$hCD34$^+$hCD38$^-$hCD90$^+$Lin$^-$ BM HSCs into NOD/SCID/IL2rγ^{null} newborns. Donor-derived viable human cells were evaluated as hCD45$^+$PI$^-$ cells. hCD33$^+$ granulocytes, hCD14$^+$ monocytes, hCD41$^+$ megakaryocytes, hCD19$^+$ B cells, hCD3$^+$ T cells, and hCD56$^+$ NK cells were detected in the BM of recipient mice. *D*, Stem and progenitor analyses of BM from mice reconstituted with hFlt3$^+$ HSCs. The BM contained hFlt3$^+$hCD34$^+$hCD38$^-$ HSCs, and all types of myeloid progenitors within the hCD34$^+$hCD38$^+$ population, including hCD45RA$^-$hCD123^{low} CMPs, hCD45RA$^+$hCD123^{low} GMPs, and hCD45RA$^-$hCD123$^-$ MEPs. The expression patterns of hFlt3 in each population were identical with those of freshly isolated stem and progenitor cells. A representative experiment by using BM samples from three independent normal donors is shown.

serum-free liquid culture, using Annexin V and PI staining (BD Pharmingen). The sorted cells were cultured in the serum-free medium (STEMPRO-34 SFM; Invitrogen) with or without FL (20 ng/ml) and/or SCF (20 ng/ml) for 24 h. The living cells were defined as Annexin V$^-$/PI$^-$ among the live-gated cells (as shown in Fig. 5*B*). For the cytokine stimulation assays, cells were sorted in the IMDM and then the cytokines were added.

In vivo assays to determine the differentiation potential and reconstitution capacity

The NOD.Cg-Prkdc^{scid}IL-2rg^{tmlWjl}/Sz (NOD/SCID/IL2rγ^{null}) mice were developed at The Jackson Laboratory. The NOD/SCID/IL2rγ^{null} strain was established by backcrossing a complete null mutation at γc locus (36) onto the NOD.Cg-Prkdc^{scid} strain. The establishment of this mouse line has been reported elsewhere (37). For the reconstitution assays, the sorted cells were transplanted into irradiated (100cGy) NOD/SCID/IL2rγ^{null} newborns via a facial vein within 48 h of birth. To confirm the long-term reconstitution by hHSCs, the chimerism of circulating human blood cells were analyzed until at least 24 wk after transplantation, as previously reported (33). In addition to the Abs described above, the following mAbs were used: allophycocyanin-conjugated anti-hCD45 (J33), PE-Cy7-conjugated anti-hCD123 (6H6), FITC-conjugated anti-hCD33 (HIM3–4) or hCD14 (M5E2), and PE-conjugated anti-hCD41 (VIPL3), hCD56 (B159), anti-hGlycophorin A (GPA) (GA-R2), or anti-hCD3 (HIT3a).

Quantitative real-time PCR

To examine the gene expression profile of each population, RNA was isolated from 2,000-sorted cells using Isogen reagent (Nippon gene) according to the manufacturer's instructions. The total RNA was reverse transcribed to cDNA using a TaKaRa RNA PCR kit (Takara Shuzo). The mRNA levels were quantified in triplicate using a real-time PCR (7500 Real-Time PCR system; Applied Biosystems). hβ2-microglobulin mRNA was separately amplified in the same plate to be used for internal control. The primer and probes were designed by Primer Express software (Applied Biosystems).

Results

The hCD34$^+$hCD38$^-$ HSC fraction express hFlt3 at a low level in both BM and CB

The hCD34$^+$Lin$^-$ population was divided into hCD38$^+$ and hCD38$^-$ populations (Fig. 1, *A* and *B*). It has been shown that HSCs with long-term reconstitution activity reside in the hCD38$^-$ fraction within the hCD34$^+$ BM and CB populations (9, 10). As shown in Fig. 1*A*, in the BM, hCD38$^-$ cells constituted only ~5% of the Lin$^-$hCD34$^+$ population. This population uniformly expressed hFlt3 at a low level. More than

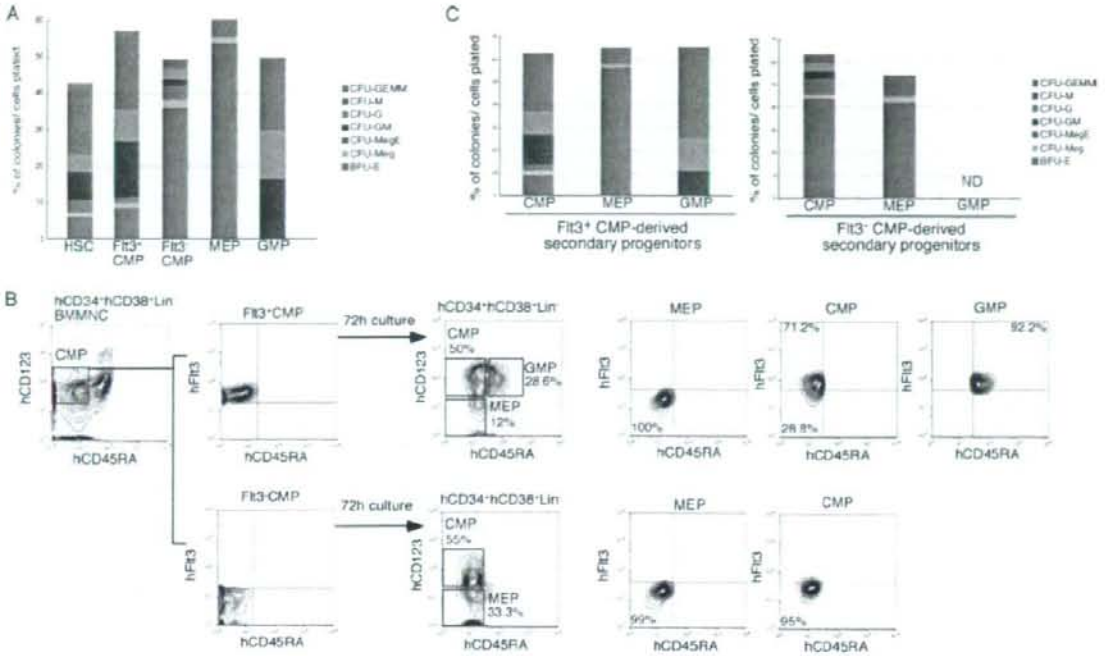

FIGURE 4. The lineage potential and the relationship of myeloid progenitor populations. *A*, Clonogenic colony formation of purified populations on methylcellulose in the presence of cytokine mixture. The hCD34$^+$hCD38$^-$ HSCs and hFlt3$^+$CMPs gave rise to various myeloid colonies including CFU-GEMM, whereas GMPs and MEPs formed exclusively GM and MegE lineage-related colonies, respectively. In contrast, hFlt3$^-$CMPs predominantly gave rise to MegE lineage-related colonies but failed to form CFU-GEMM. The mean value of eight independent experiments is shown. CFU-M: CFU-macrophage, CFU-G: CFU-granulocyte, CFU-GM: CFU-granulocyte/macrophage, CFU-MegE: CFU-megakaryocyte/erythroid, CFU-Meg: CFU-megakaryocyte, and BFU-E: burst-forming units-erythroid. *B*, The lineal relationship between hFlt3$^+$CMPs and hFlt3$^-$CMPs. After 72 h of culturing, hFlt3$^+$CMPs gave rise to hFlt3$^-$CMPs, GMPs, and MEPs. In contrast, hFlt3$^-$CMPs differentiated into only MEPs, thus suggesting hFlt3$^-$CMP to be a transitional intermediate population from hFlt3$^+$CMPs to hFlt3$^-$MEPs. *C*, The colony formation activity of phenotypically defined secondary CMPs, GMPs, and MEPs purified from the primary culture of hFlt3$^+$CMPs or hFlt3$^-$CMPs. Each population displayed the colony formation activity consistent with their phenotypic definition. The mean value of four independent experiments is shown.

60% of the hCD34$^+$hCD38$^-$ BM cells also expressed hCD90, another critical marker for hHSCs (11–13), whereas the hCD34$^+$hCD38$^+$Lin$^-$ fraction was constituted of hCD90$^-$ lineage-committed progenitors.

In the CB, only ~30% of hCD34$^+$hCD38$^-$ cells expressed hCD90 (Fig. 1*B*). In the NOD/SCID/IL2rγ^{null} newborn system, the hCD34$^+$hCD38$^-$hCD90$^+$ population was highly enriched for HSCs capable of long-term reconstitution as compared with the hCD34$^+$hCD38$^-$hCD90$^-$ CB fraction (F. Ishikawa, unpublished data). The vast majority of hCD34$^+$hCD38$^-$ cells expressed hFlt3 at a low level as previously reported (38). Furthermore, the hCD34$^+$hCD38$^-$hCD90$^+$ CB population expressed hFlt3.

These data clearly show that hFlt3 is expressed in all cells with the hHSC phenotype in both the BM and the CB, and suggest that Flt3 expression does not discriminate ST-HSCs from LT-HSCs in human as it does in mouse (16, 17). In contrast, the BM and the CB hCD34$^+$hCD38$^+$ progenitor fraction expressed negative to high levels of hFlt3. We thus further subfractionated the hCD34$^+$hCD38$^+$ population to evaluate the hFlt3 expression in a variety of lineage-restricted progenitors.

The expression of hFlt3 within the hCD34$^+$hCD38$^+$ progenitor fraction

In mouse hematopoiesis, the expression of mFlt3 is associated with early lymphoid progenitor activities; it is expressed in the majority of CLPs, and in the minority of CMPs with weak B cell potential (20), but not in MEPs or GMPs (20) (21). Fig. 2 shows the expression of hFlt3 in the myeloid and lymphoid progenitor populations. According to the phenotypic definition of human myeloid and lymphoid progenitors (14, 15, 39, 40), hCD34$^+$hCD38$^+$ cells were subfractionated into myeloid and lymphoid progenitors, including the hCD45RA$^-$hCD123 (IL-3Rα)^{low} CMP, the hCD45RA$^-$hCD123$^-$ MEP, the hCD45RA$^+$hCD123^{low} GMP, the hCD10$^+$hCD19$^-$ CLP, and the hCD10$^+$hCD19$^+$proB populations. Interestingly, in both the human BM and CB, ~70–80% of CMPs expressed hFlt3, whose level was progressively up-regulated at the GMP stage. In contrast, hFlt3 expression was completely shut down in MEPs. In the lymphoid lineage, the hCD34$^+$hCD38$^+$hCD10$^+$ CLP (15) strongly expressed hFlt3, whereas hFlt3 was down-regulated in the proB cells. The expression level of hFlt3 in GMPs and CLPs appears to be higher than that in hCD34$^+$hCD38$^-$hCD90$^+$ HSCs (Fig. 2). We also tested the level of hFlt3 transcripts in purified hBM HSCs and progenitor populations (Fig. 3*A*). The pattern of hFlt3 mRNA expression was generally consistent with that in hFlt3 protein, as evaluated by using anti-hFlt3 Abs on FACS (Figs. 1 and 2). Consistent with a previous report (41), MEPs and hFlt3$^-$ CMPs had the lowest levels, GMPs and CLPs had the highest levels, and the hCD34$^+$hCD38$^-$ HSC population had a medium level of hFlt3 mRNA. Collectively, functional hLT-HSCs express hFlt3 mRNA

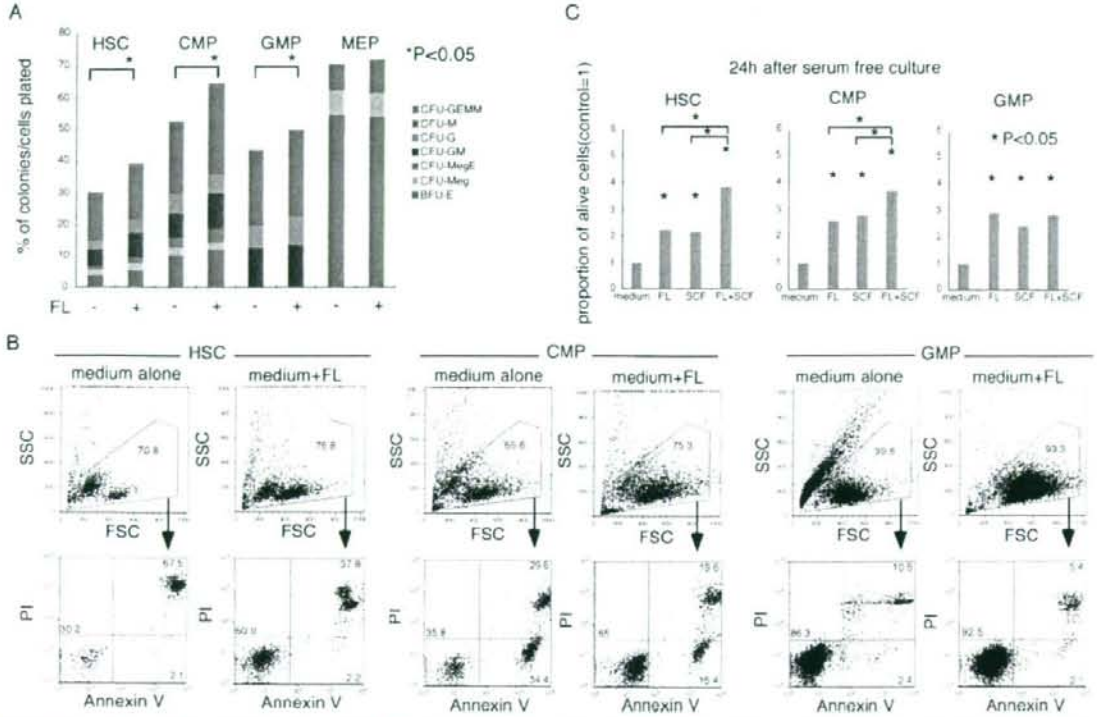

FIGURE 5. Effect of FL and SCF on the survival of purified progenitors. *A*, The effect of additional FL on colony formation of purified progenitors in methylcellulose in the presence of SCF, IL-3, IL-11, GM-CSF, Epo, and Tpo. Results from five independent experiments are shown here. Note that colony numbers are increased by the addition of FL into cultures in all hFlt3-expressing subsets including HSCs, CMPs, and GMPs but not in hFlt3$^-$ MEPs. *B*, An evaluation of apoptotic cell death in cultures of stem and progenitor cells. HSCs, hFlt3$^+$ CMPs, and GMPs were cultured in the serum-free media, with or without FL, and analyzed at 12, 18, 24, 30, 48, and 72 h after initiation of culture. A representative data obtained after 24-h culture is shown. *C*, Anti-apoptotic effects of FL and/or SCF on HSCs and Flt3$^+$ CMPs. Annexin$^-$ PI$^-$ live cells were enumerated after 24-h culture in a serum-free media. Each graph shows n-fold differences in the percentage of live cells relative to the ones without cytokine. Each bar represents the mean value and the SD of five independent samples.

and surface protein, and the distribution of Flt3 is quite different between human and mouse in early hematopoiesis.

In contrast, c-Kit was expressed at high levels in human HSCs and myelo-erythroid progenitors, while at a low level in CLPs (Fig. 1*C*). The expression pattern of c-Kit in human hematopoietic stem and progenitor cells is generally consistent with that in mouse hematopoiesis (4, 6, 7), suggesting that the c-Kit expression program is preserved in mouse and human hematopoiesis.

hFlt3 is expressed in functional hHSCs capable of reconstituting normal hematopoiesis in the NOD/SCID/IL-2 receptor γ-chain null (NOD/SCID/IL2rγ^{null}) mouse model

In the NOD/SCID/IL2rγ^{null} newborn system, hCD34$^+$hCD38$^-$ BM and CB cells are capable of reconstitution of all hematopoietic lineages for a long term (33). The entire hCD34$^+$hCD38$^-$ BM population expressed hFlt3 (Fig. 1*A*), suggesting that functional hBM HSCs possess hFlt3 on their surface. In contrast, hCD34$^+$hCD38$^-$ CB cells contained some hCD90$^-$ cells that did not express hFlt3. To formally test whether Flt3-expressing hCD34$^+$hCD38$^-$ CB cells possess LT-HSC activity, we transplanted hFlt3$^+$hCD34$^+$hCD38$^-$hCD90$^+$ CB cells in to NOD/SCID/IL2rγ^{null} newborns. As shown in Fig. 3*B*, NOD/SCID/IL2rγ^{null} mice transplanted with 1×10^3 hFlt3$^+$hCD34$^+$hCD38$^-$hCD90$^+$ CB cells reconstituted all hematolymphoid lineages for >6 mo, indicating that hFlt3 is expressed in functional hHSCs in CB as well as in BM.

Fig. 3*C* shows the phenotypic analysis of human progeny from 5×10^3 hFlt3$^+$hCD34$^+$hCD38$^-$hCD90$^+$ BM cells 6 (*upper panels*) or 15 wk (*lower panels*) after transplantation into NOD/SCID/IL2rγ^{null} newborns (33). hFlt3$^+$hCD34$^+$hCD38$^-$hCD90$^+$ BM cells differentiated into all hematopoietic lineage cells, including hCD33$^+$ granulocytes, hCD14$^+$ monocytes, hCD41$^+$ megakaryocytes, hCD19$^+$ B cells, hCD3$^+$ T cells, hCD56$^+$ NK cells (Fig. 3*C*), and hGPA$^+$ erythrocytes (not shown). Furthermore, transplanted hFlt3$^+$hCD34$^+$hCD38$^-$ HSCs purified from primary recipients developed secondary hFlt3$^+$ HSCs and hFlt3$^{-/+}$ CMPs, hFlt3$^-$ MEPs, and hFlt3$^+$ GMPs recapitulating normal human hematopoietic development. Thus, the hCD34$^+$hCD38$^-$hCD90$^+$ BM population contains cells with long-term SCID reconstitution potential as reported (33, 42), and all cells within this population express hFlt3 on their surface (Fig. 3*D*).

The up- or down-regulation of hFlt3 in the myeloid pathway is associated with GM or MegE differentiation activity, respectively

Fig. 4*A* shows the differentiation potential of purified BM progenitors in vitro in the presence of the myeloid cytokine mixture containing SCF, FL, IL-3, IL-11, Tpo, Epo, and GM-CSF. hFlt3$^+$

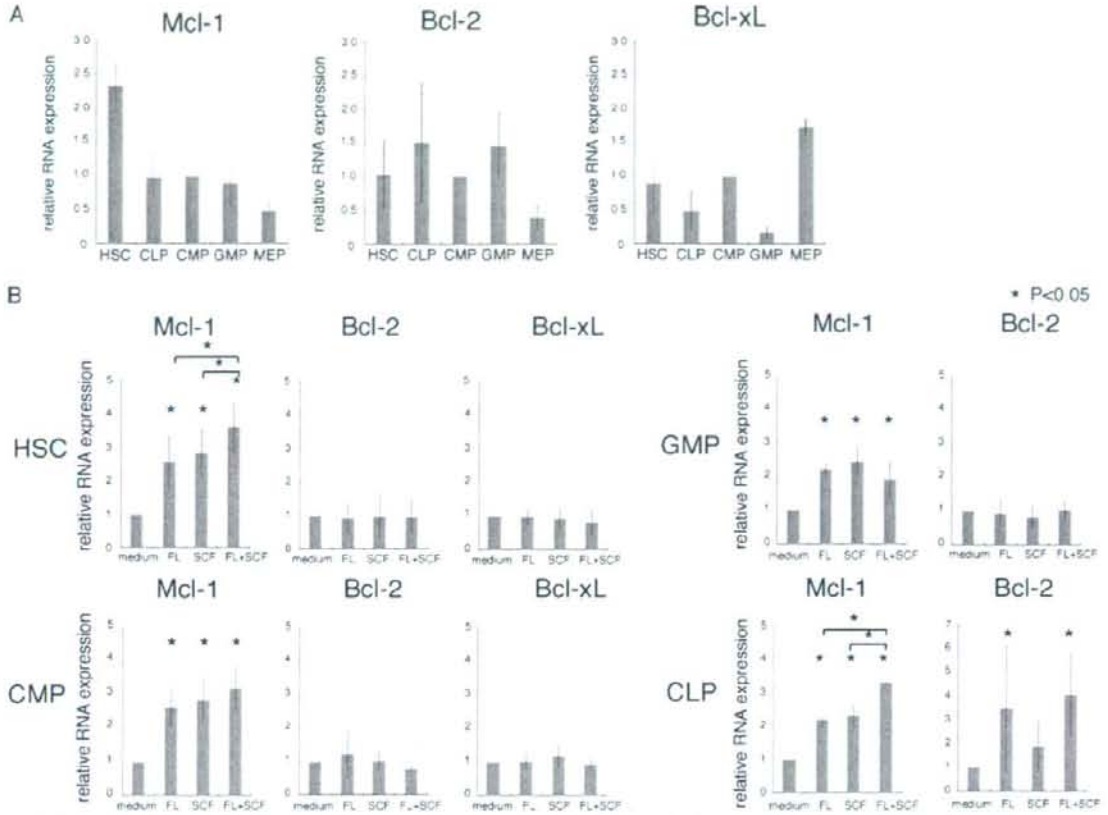

FIGURE 6. *A*, Quantitative RT-PCR assays for human anti-apoptotic genes such as Mcl-1, Bcl-2, and Bcl-x_L in purified HSCs and each progenitor population. Each bar represents an *n*-fold difference in the amount of anti-apoptotic gene expression relative to that in Flt3$^+$ CMPs. Note that Mcl-1 expression level is highest in HSCs, whereas Bcl-2 and Bcl-x_L expression is most pronounced in GMPs and MEPs, respectively. *B*, Changes in anti-apoptotic gene expression in each progenitor after incubation with FL and/or SCF. Significant up-regulation of Mcl-1 mRNA was seen in HSCs, Flt3$^+$ CMPs, GMPs, and CLPs after incubation with FL and/or SCF. Each bar represents the mean value and the SD of sixe independent samples.

CMPs formed a variety of myelo-erythroid colonies including clonogenic CFU-granulocyte/erythroid/macrophage/megakaryocyte (CFU-GEMM), whereas hFlt3$^-$ CMPs did not form CFU-GEMM, but preferentially differentiated into the MegE lineage. Since GMPs (hFlt3$^+$) and MEPs (hFlt3$^-$) exclusively gave rise to GM- and MegE-related colonies, respectively, hFlt3 expression could be associated with GM lineage development. These results suggested that hFlt3$^+$ CMPs might differentiate into MEPs via hFlt3$^-$ CMPs. We thus directly tested the lineage relationship of these purified myelo-erythroid progenitor populations (Fig. 4*B*). hFlt3$^+$ and hFlt3$^-$ CMPs were purified and cultured in vitro. Then, 72 h after the initiation of culture, hFlt3$^+$ CMPs gave rise to hFlt3$^-$ CMPs, hFlt3$^+$ GMPs and hFlt3$^-$ MEPs, whereas hFlt3$^-$ CMPs did not up-regulate hFlt3, differentiating only into hFlt3$^-$ MEPs. Such phenotypically defined secondary myeloid progenitors displayed differentiation activity consistent with their phenotypic definition (Fig. 4*C*). These data suggest that multipotent hFlt3$^+$ CMPs can differentiate into both GMPs and MEPs, whereas hFlt3$^-$ CMPs represent a transitional stage into MEPs.

Flt3 signaling protects human hematopoietic stem and progenitor cells from apoptotic cell death

We wished to elucidate the role of Flt3 signaling in human hematopoiesis. We first tested the effect of Flt3 signaling on the differentiation of HSCs, CMPs, and GMPs. Purified hFlt3$^+$ HSCs, CMPs, and GMPs were cultured in methylcellulose in the presence of the myeloid cytokine mixture, with or without hFL. As shown in Fig. 5*A*, the addition of FL in the culture did not affect the percentage of GM, MegE, or mix colonies in any of these populations. Interestingly, however, the colony numbers significantly increased in all cases when FL was added to the culture. This effect was dose-dependent, and the stimulatory activity of FL reached its peak at a concentration of 5 ng/ml (not shown). The plating efficiencies of hFlt3$^+$ HSCs, CMPs, and GMPs cultured with the cytokine mixture containing FL (20 ng/ml) were significantly higher than those cultured without FL, suggesting that FL signaling may enhance the viability of cells (Fig. 5*A*). We then directly tested the viability of HSCs, CMPs, and GMPs 24 h after the initiation of culture in serum-free media, with or without FL. The live, apoptotic, and dead cells after culture were enumerated by the Annexin/PI staining (43). In this staining, live cells are Annexin$^-$/PI$^-$, whereas Annexin$^+$/PI$^-$ and Annexin$^+$/PI$^+$ cells are apoptotic and dead cells, respectively (Fig. 5*B*). Without FL, a considerable proportion of purified HSCs, CMPs, and GMPs rapidly became Annexin$^+$/PI$^-$ and Annexin$^+$/PI$^+$ cells undergoing apoptotic cell death. The addition of FL significantly blocked apoptotic cell death in all of these populations, indicating that FL plays a critical role in human hematopoietic stem and progenitor cell survival (Fig.

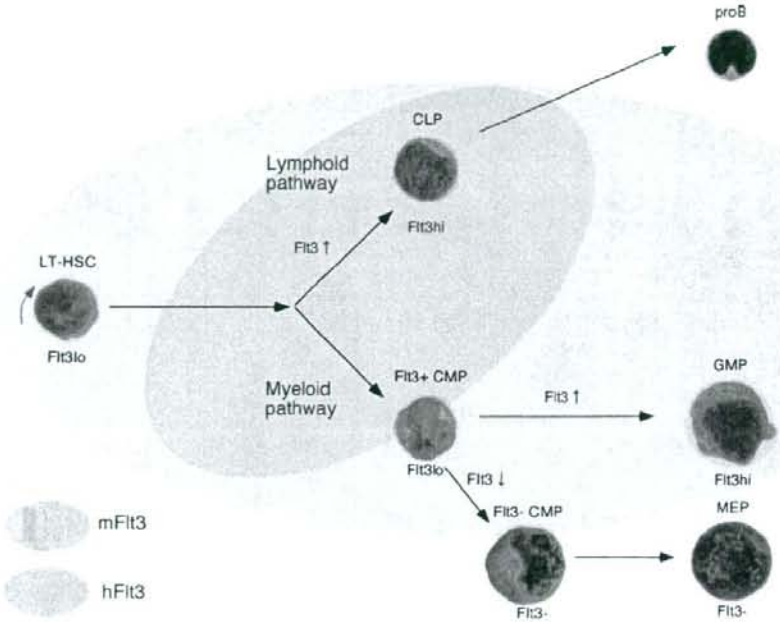

FIGURE 7. Proposed differential expression of human and mouse Flt3 in steady-state hematopoiesis. Cellular morphology of directly sorted each progenitors (May-Giemsa ×1000) is shown here. In human, the most primitive LT-HSC expressed hFlt3 at a low level and its expression is up-regulated at the early GM and the lymphoid progenitor stages, while it is down-regulated in MEPs. In contrast, the mouse LT-HSC lacks mFlt3 expression, and mFlt3 is expressed in cells primed to the lymphoid pathway, including CLPs and a fraction of CMPs.

5*B*). These data strongly suggest that Flt3 signaling does not instruct hematopoietic lineage commitment in hFlt3-expressing myeloid progenitors, but it does promote their survival.

SCF, the ligand for c-Kit, has also been shown to play a critical role in the maintenance of survival in early hematopoiesis. Both c-Kit and Flt3 belong to the class III receptor tyrosine kinase (RTK) family, sharing their major signaling cascade (44). Human HSCs, CMPs, and GMPs expressed both c-Kit and Flt3 at the single cell level (Fig. 1). Thus, we tested the anti-apoptotic effect of SCF in this system. As shown in Fig. 5*C*, in all HSC, CMP, and GMP populations, SCF also displayed anti-apoptotic effects whose impact on cell survival is similar to that of FL. Furthermore, in HSCs and CMPs, the combination of FL and SCF further increased percentages of live cells as compared with those in the presence of either FL or SCF alone, suggesting that SCF and FL signals collaborate to maintain cell survival of HSCs and CMPs.

Flt3 signaling up-regulates Mcl-1, but not Bcl-2 or Bcl-x_L, expression in human hematopoietic stem and progenitor cells

The question: is the mechanism of cell survival enhancement by signaling of RTKs, such as Flt3 and c-Kit? We have shown that in murine hematopoiesis, Mcl-1, a Bcl-2 homologue, is indispensable for hematopoietic stem and progenitor cell survival, and that c-Kit signaling is one of the most critical inducers for Mcl-1 expression in mHSCs (45). We therefore hypothesized that Flt3, as well as c-Kit, signaling may up-regulate Mcl-1 to maintain cell survival in human hematopoiesis as well.

Fig. 6*A* shows the distribution of the transcripts of Bcl-2 family molecules including Mcl-1, Bcl-2, and Bcl-x_L in human stem and progenitor cells. Mcl-1 is expressed at the highest level in HSCs. CMPs and CLPs expressed similar levels of Mcl-1, and MEPs expressed Mcl-1 at the lowest level. This expression pattern of Mcl-1 transcript in human hematopoiesis is consistent with that in murine hematopoiesis (45). In contrast, Bcl-2 was highly expressed in GMPs and CLPs, whereas Bcl-x_L was expressed in MEPs at the highest level.

Purified stem and progenitor populations were incubated with FL and/or SCF in serum-free media. Both FL and SCF dramatically up-regulated the expression of Mcl-1 in a dose-dependent manner, and it reached its peak 30 min after initiation of culture at a concentration of 5 ng/ml (data not shown). Fig. 6*B* shows the relative expression level of Mcl-1, Bcl-2, and Bcl-x_L in the presence of 20 ng/ml FL and/or SCF. We found that both FL and SCF significantly up-regulated the expression of Mcl-1, but not of Bcl-2 or Bcl-x_L, in HSCs, CMPs, and GMPs. These data collectively suggest that one of the important functions of these class III RTKs is to specifically activate Mcl-1 expression. Interestingly, in HSCs, FL and SCF displayed an additive effect on the up-regulation of Mcl-1. Therefore, Flt3 and c-Kit signaling collaborate to protect $Flt3^+$ HSCs and early myeloid progenitors from apoptotic cell death, presumably through activating anti-apoptotic Mcl-1 transcription. In CLPs, however, FL activated not only Mcl-1 but also Bcl-2 transcription.

Discussion

In this study, by using a multicolor FACS and a highly efficient xenograft system, we provide evidence that the distribution of Flt3 RTK is quite different in human and mouse hematopoiesis. First, although mouse LT-HSCs do not express mFlt3, the HSC-enriched $hCD34^+hCD38^-hLin^-$ population, that can reconstitute human hematopoiesis for a long-term in our xenogenic mouse model, uniformly expresses hFlt3 in both BM and CB. It is still unclear whether SCID-repopulating cells directly correspond to hLT-HSCs. However, because the $hCD34^+hCD38^+hLin^-$ cells never